THE JOURNAL OF BIOLOGICAL CHEMISTRY VOL. 290, NO. 3, pp. 1456–1473, January 16, 2015

Vitamin A Deficiency Causes Hyperglycemia and Loss of Pancreatic β-Cell Mass*

Received for publication, October 6, 2014, and in revised form, November 24, 2014 Published, JBC Papers in Press, December 1, 2014, DOI 10.1074/jbc.M114.616763

Steven E. Trasino, Yannick D. Benoit, and Lorraine J. Gudas[1]

From the Department of Pharmacology, Weill Cornell Medical College, New York, New York 10065

Background: Little is known about vitamin A (VA) regulation of pancreatic endocrine mass in adults.
Results: Decreased pancreatic VA causes increased α-cell to β-cell mass ratios, hyperglycemia, and hyperglucagonemia. Reintroducing dietary VA restores normoglycemia and α-cell to β-cell mass.
Conclusion: VA is essential for maintenance of β-cell functions in adult pancreas.
Significance: VA therapies may potentially prevent β-cell apoptosis and loss in diabetes.

We show that vitamin A (all-*trans*-retinol) (VA) is required both for the maintenance of pancreatic β-cell and α-cell mass and for glucose-stimulated insulin secretion in adult mice. Dietary VA deprivation (VAD) causes greatly decreased pancreatic VA levels, hyperglycemia, and reduced insulin secretion. Adult mice fed VAD diets display remodeling of the endocrine pancreas, marked β-cell apoptosis, shifts to smaller islet size distributions, decreased β-cell mass, increased α-cell mass, and hyperglucagonemia. Importantly, although we induced VAD in the entire animal, the pancreatic β-cells are exquisitely sensitive to VAD-associated apoptosis compared with other cell types in other organs. VAD causes major reductions in levels of the VA intracellular binding protein Crbp1 and the retinoic acid-metabolizing enzyme Cyp26a1 specifically in larger islets, suggesting the use of these proteins as biomarkers for early endocrine mass abnormalities. In the VAD mice, the reductions in pancreatic islet sizes and the associated aberrant endocrine functions, which show similarities to the phenotype in advanced type 2 diabetes, result from reductions in pancreatic VA signaling. Reintroduction of dietary VA to VAD mice restores pancreatic VA levels, glycemic control, normal islet size distributions, β-cell to α-cell ratios, endocrine hormone profiles, and RARβ2 and RARγ2 transcript levels. Restoration of β-cell mass by reintroducing VA to VAD mice does not involve increased β-cell proliferation or neogenesis. Pharmacologic modulation of pancreatic VA signaling should be explored for the preservation and/or restoration of pancreatic β-cell mass and function in individuals with diabetes mellitus.

Vitamin A (VA, all-*trans*-retinol (ROL))[2] and its analogs and metabolites are collectively called retinoids (1). Acting through the retinoic acid receptors (RARα, β, and γ), all-*trans*-retinoic acid, a biologically active metabolite of VA, is essential for embryonic stem cell differentiation (1, 2) and is required during early vertebrate pancreatic specification and in later stages of pancreagenesis when β-cell determination and maturation occur (3–5). 9-*cis*-Retinoic acid has been shown to have a role in the adult pancreas (6), and we recently demonstrated that when embryonic stem cells that lack RARβ are subjected to an endocrine cell differentiation protocol, they show both reduced levels of markers of pancreatic progenitors, such as neurogenin-3 (ngn3), and reduced differentiation into insulin-positive endocrine cells (7). These data led us to hypothesize that retinoids play an essential role in the maintenance of endocrine cell populations in the adult pancreas. Although Chertow *et al.* (8, 9) demonstrated that perfused islets from VA-deprived rats had impaired insulin and glucagon secretion, in these studies the fetuses were deprived of VA. This VA deprivation caused pancreatic developmental abnormalities in the pups (10), making it likely that the pancreatic phenotype resulted from the pancreatic abnormalities shown to be associated with low VA levels during embryogenesis and early development (10).

Here we demonstrate for the first time that decreases in pancreatic levels of VA in adult mice result in loss of β-cell mass, increased α-cell mass with concomitant hyperglycemia, and changes to serum insulin and glucagon profiles. These alterations in islet architecture and pancreatic endocrine cell types, serum hormones levels, and hyperglycemia in VA-deprived mice are reversed upon resumption of dietary VA. Because of the clinical interest in the development of pancreatic β-cell mass restoration therapy for T2D and type 1 diabetes (11), the data reported here suggest that pancreatic VA metabolism and signaling should be further explored for endocrine cell restoration therapies in diabetes mellitus.

EXPERIMENTAL PROCEDURES

Animals and Vitamin A-deficient Diets—Details on how lecithin retinol acyltransferase null ($LRAT^{-/-}$) mice, a genetically modified model of impaired VA storage, were generated can be read in Ref. 12. Briefly, $LRAT^{-/-}$ knock-out mice were produced on a C57BL/6 background and lack the enzyme lecithin retinol acyltransferase, which is the primary enzyme responsible for esterifying dietary VA (retinol). Compared with WT,

* This work was supported, in whole or in part, by National Institutes of Health Grants R01CA043796 and RO1 DE010389 (to L. J. G.) and CA062948 (to S. E. T.). This work was also supported by Weill Cornell funds.

[1] To whom correspondence should be addressed: Dept. of Pharmacology, and Weill Cornell Medical College of Cornell University, 1300 York Ave., New York, NY 10065. Tel.: 212-746-6250; Fax: 212-746-8858; E-mail: ljgudas@med.cornell.edu.

[2] The abbreviations used are: VA, vitamin A; VAD, vitamin A-deficient or VA deprivation; ROL, all-*trans*-retinol; RA, retinoic acid; T2D, type 2 diabetes; RAR, retinoic acid receptor; VAS, VA-sufficient; VADR, VAD rescued; GTT, glucose tolerance test; LRAT, lecithin:retinol acyltransferase; PSC, pancreatic stellate cell; ngn3, neurogenin-3.

TABLE 1
Gene expression primers primers

Gene name (alias)	Gene ID	Forward primer (5′ → 3′)	Reverse primer (5′ → 3′)
RARα	19401	CCATGTACGAGAGTGTGGAAGTC	CCTGGTGCGCTTTGCGA
RARβ2	218772	GATCCTGGATTTCTACACCG	CACTGACGCCATAGTGGTA
RARγ2	19411	TGGCCACCAATAAGGAGAGACT	GATACAGTTTTTGTCACGGTGACAT
RXRα	20181	ATGGACACCAAACATTTCCTGC	CCAGTGGAGAGCCGATTCC
Crbp1(Rbp1)	19659	GCTGAGCACTTTTCGGAACT	GGAGTTTGTCACCATCCCAG
Crabp1(Rbp5)	12903	AAGGCGTTGGGTGTGAACGC	TGCGTCCGTCCACTGTCTCCT
Crabp2	12904	CTTGCTGCCACTATGCCTAA	TGTTTGATCTCGACTGCTGG
Cyp26A1	13082	GAAACATTGCAGATGGTGCTTCAG	CGGCTGAAGGCCTGCATAATCAC
Ins1	16333	GCAAGCAGGTCATTGTTTCA	GGTGGGCCTTAGTTGCAGTA
Ins2	16334	AAGCCTATCTTCCAGGTTATT	TGGGTCCTCCACTTCACG
Pygl	110095	CTATGGCTACGGCATTCGTT	AAGGGTTTCCATGCCTGAG
Hprt	15452	GCTTGCTGGTGAAAAGGACCTCTCGAAG	CCCTGAAGTACTCATTATAGTCAAGGGCAT
36B4	11837	AGAACAACCCAGCTCTGGAGAAA	ACACCCTCCAGAAAGCGAGAGT

$LRAT^{-/-}$ mice show substantially more depleted VA levels in many tissues when fed a VA-deficient diet because they cannot store VA (12). WT C57BL/6 male mice (Jackson Laboratory, Bar Harbor, ME) and $LRAT^{-/-}$ male mice were housed with five mice per cage with a 12-h light/dark cycle with free access to food and water.

VA Deprivation—Dietary VA deprivation studies were performed on 6-week-old male WT and $LRAT^{-/-}$ mice as previously described (12). The numbers of mice per experimental group and timelines are outlined in Fig. 1*A*. Briefly, WT and $LRAT^{-/-}$ mice were randomly placed on either a VA-sufficient (VAS) control diet (#88406; Harlan, Madison, WI; retinyl palmitate = 20 IU/gram) or a VAD diet (Harlan #88407) for 4 or 10 weeks (w). After 4 and 10 weeks, we subjected cohorts of mice to metabolic testing, and we collected tissue and serum samples in the dark and stored them at −70 °C for further analysis. For VA rescue experiments, cohorts of WT and $LRAT^{-/-}$ mice deprived of VA for 10 weeks were switched back to a VAS diet (#88406; retinyl palmitate = 20 IU/gram) for an additional 8 weeks, subjected to metabolic testing, and sacrificed, and tissue and serum samples were collected and stored at −70 °C. All experiments were repeated a minimum of three times ($n = 3$) with $n = 4–7$ mice per group in each experiment. WT and $LRAT^{-/-}$ mice fed the VAS and VAD diets for 4 weeks are referred to as 4wVAS and 4wVAD, respectively, and mice fed the VAS and VAD diets for 10 weeks are referred to as 10wVAS and 10wVAD. Cohorts of mice deprived of VA for 10 weeks ($n = 5$) and then returned to a VAS diet for 8 weeks are referred to as VAD rescued (VADR) mice.

HPLC of Pancreatic Retinol—Pancreas retinol was extracted and analyzed as described (12). Briefly, 350 μl of acetonitrile: butanol (50:50, v/v) and 0.1% butylated hydroxytoluene were added to 0.5 ml of homogenized pancreatic tissue. The mixture was vortexed thoroughly for 30 s. After addition of 300 μl of a saturated K_2HPO_4 solution and thorough mixing, the samples were centrifuged for 10 min at 12,000 × *g*. The upper organic layer containing retinoids was collected. Retinoid samples (200 μl) were loaded on an analytical 5-μm reverse phase C18 column (Vydac, Hesperia, CA) and eluted at a flow rate of 1.5 ml/min using a Waters Millennium system (Waters Corp., Milford, MA) automated HPLC system. Retinol was detected at a wavelength of 340 nm and identified by a match of the 32.1-min retention time of a pure ROL standard. We measured extraction efficiency by using retinyl acetate, which, as an internal standard, eluted at 37.3 min. The concentration of the ROL standard and extraction efficiency were used to calculate pancreatic tissue ROL concentrations normalized to mg of wet tissue.

Metabolic Measurements—Glucose tolerance was performed using an intraperitoneal glucose tolerance test (GTT) as previously described (13). Mice were fasted overnight followed by intraperitoneal injections ($n = 5$ per group) of 50% glucose in PBS at 2.0 g of glucose/kg of body weight. Tail vein blood was collected at 15, 30, 45, 60, and 120 min postinjection for glucose measurements using a FreeStyle Lite blood glucose monitoring system (Abbott Diabetes Care, Inc., Alameda, CA). Insulin tolerance tests were performed on WT and $LRAT^{-/-}$ VA sufficient and $LRAT^{-/-}$ VA-deficient mice as previously described (14). WT and $LRAT^{-/-}$ mice were fasted for 3 h followed by intraperitoneal injections with insulin (Humulin R; Eli Lilly, 2 units/kg of body weight). Tail vein blood glucose was measured at 20, 40, 60, and 120 min after injection using a FreeStyle Lite blood glucose monitoring system (Abbott Diabetes Care, Inc.). To determine insulin secretion responses to glucose, serum fractions were isolated between 0 and 60 min after glucose injections and insulin concentrations were measured using an Ultrasensitive insulin ELISA kit (Alpco, Inc., Salem, NH). Random blood glucose measurements were taken from tail veins of 7–10 mice per group at two or three random time points daily after 4 and 10 weeks of VA deprivation. Serum glucagon was measured using a glucagon Quantikine ELISA Kit (R&D Systems). The means are expressed as ± S.E., and *p* values were calculated using one-way analysis of variance followed by Bonferroni post hoc analysis.

RNA Isolation and cDNA Synthesis—Total RNA was isolated from whole pancreas and small intestine homogenates using RNeasy mini kits (Qiagen) and quantified using a Nano Drop 2000 spectrophotometer (Thermo Scientific, Wilmington, DE). Total RNA (2 μg) was used to synthesize cDNA with random primers using a qScript cDNA synthesis kit (Quanta Biosciences, Gaithersburg, MD).

Semiquantitative and Quantitative RT-PCR—Quantitative RT-PCR was performed using SYBR Green PCR master mix on a Bio-Rad MyiQ2 Real Time PCR iCycler (Bio-Rad). Gene specific primers (Table 1) were used to amplify mRNA of target genes, which were normalized to either *36b4* or *Hprt* internal control genes. cDNA from 5–7 mice per experimental group was analyzed for relative mRNA fold changes, calculated using

the Pfaffl method (15). For semiquantitative PCR of genes, PCR amplification of target genes was completed within the linear range, and ethidium bromide-stained PCR products were resolved on 2% agarose gels and visualized under UV light. cDNA from the rodent β-cell cell line, INS-1E, was used a positive control for the PCR of *ins1* and *ins2* genes. Relative gene expression values are reported as means ± S.E., and *p* values were calculated using two-way analysis of variance followed by Bonferroni multiple comparison test post hoc analysis.

Pancreatic Insulin and Glucagon Measurements—Pancreatic insulin and glucagon levels were measured in lysates from pancreatic tissues using an ultrasensitive insulin ELISA kit (Alpco, Inc.) and glucagon quantikine ELISA kit (R&D Systems) as per the manufacturers' instructions. Insulin and glucagon concentrations were normalized to pancreatic protein concentrations determined using the DC protein assay (Bio-Rad) according to the manufacturer's protocol. Endocrine hormones levels are reported as means ± S.E., and *p* values calculated using two-way analysis of variance followed by Bonferroni multiple comparison test post hoc analysis.

Immunofluorescence and Immunostaining Microscopy—Paraffin-embedded or frozen pancreatic tissue sections were incubated with antibodies against: C-peptide (rabbit polyclonal, 1:300, catalog no. 4593, Cell Signaling, Danvers, MA), insulin (mouse monoclonal 1:300, #1061, Beta Cell Biology Consortium), glucagon (mouse monoclonal, 1:300, ab82270, Abcam, Cambridge, MA), glucagon (1:300, rabbit polyclonal #sc-13091, Santa Cruz, Santa Cruz, CA), Crbp1 (RBP1) (mouse monoclonal, 1:300, sc-271208, Santa Cruz) Cyp26a1 (mouse monoclonal, 1:300, # sc-53618 Santa Cruz), Ki67 (rat monoclonal, 1:300, # M7249, Dako, Carpinteria, CA), proliferating cell nuclear antigen (mouse monoclonal, 1:300, #2586, Cell Signaling), Pdx1 (rabbit polyclonal, 1:500; Abcam, ab47267), neurogenin-3 (mouse monoclonal,1:200, #2013, Beta Cell Biology Consortium), Vimentin (goat polyclonal 1:500, #sc-7558, Santa Cruz), α-smooth muscle actin (mouse monoclonal 1:1000, Dako, Carpinteria, CA). We utilized Alexa Fluor 594- and 488-conjugated anti-rabbit (1:500), anti-mouse (1:500), anti-goat (1:500), and anti-rat, secondary (1:500) antibodies (Invitrogen) for immunofluorescence labeling of targets, followed by visualization using a Nikon TE2000 inverted fluorescence microscope. Pdx1 signals were visualized with a Super Picture polymer detection kit (Invitrogen).

Measurement of Pancreatic Endocrine Cell Mass and Crbp1 and Cyp26a1 Islet Expression Patterns—Pancreatic endocrine cell mass and islet Crbp1 and Cyp26a1 islet expression patterns were determined using a direct point counting method coupled with double immunofluorescence labeling (16). The entire pancreas was excised from 5–7 mice from each experimental group, weighed, fixed in 4% formaldehyde buffer, and embedded in paraffin wax. Paraffin-embedded pancreatic tissues were exhaustively sectioned at 6–7-μm thicknesses 150 μm apart, mounted on glass slides, and stained with antibody combinations of either: C-peptide (1:300) and glucagon (1:300), C-peptide (1:300) and Crbp1 (1:300), or C-peptide (1:300) and Cyp26a1 (1:300) at 4 °C for 24 h. The appropriate Alexa Fluor anti-rabbit (1:500) and Alexa Fluor anti-mouse (1:500)-conjugated secondary antibodies were used for labeling of β-cells, α-cells, and Crbp1- and Cyp26a1-positive cells, which were visualized using a using a Nikon TE2000 inverted fluorescence microscope. Between 250 and 300 immunopositive islet fields for C-peptide, glucagon, Crbp1, and Cyp26a1 were photographed per mouse and analyzed for β-cell and α-cell mass, and Crbp1- and Cyp26a1-positive areas, mean pancreatic islet areas, islet size distributions, and total numbers of islets by using Nikon NIS elements AR advanced imaging software suite (Nikon). β-Cell mass was calculated by using the following formula: β-cell mass (mg) = total C-peptide positive islet area (μm^2)/total pancreatic tissue area (μm^2) × pancreatic tissue weight (mg). Total α-cell mass was calculated by subtracting the total glucagon positive area from the total islet area and multiplying by pancreatic weight in mg. Endocrine cell mass is reported as means ± S.E., and the *p* values were calculated using two-way analysis of variance followed by Bonferroni multiple comparison test post hoc analysis.

Correlation Analysis Between Crbp1 and Cyp26a1 Islet Expression and Islet Area—The percentages of total Crbp1- and Cyp26a1-positive islet areas were measured in 250–300 islet fields per mouse in 5–7 mice per experimental group. The percentages of islet Crbp1- and Cyp26a1-positive areas were determined and, based on a total range of relative islet areas, binned within a range of either large (30,000–20,000 μm^2), medium (20,000–10,000 μm^2), or small (10,000–2,000 μm^2) islet sizes. Linear relationships between pancreatic islet size area and percentages of islet expression of Crbp1 or Cyp26a1 were determined by standard least squares regression analysis using GraphPad Prism 6.0 statistical software (GraphPad Software, San Diego, CA).

Detection of Apoptosis—Apoptosis was measured on frozen pancreatic, liver, kidney, and intestine sections using the TUNEL Apoptag *in situ* apoptosis detection kit (Millipore, Billerica, MA) and a fluorescein *in situ* cell death detection kit (Roche Life Sciences) according to the manufacturers' protocols. Apoptotic β-cells and hepatocytes were also detected by double immunofluorescence staining with antibodies against cleaved caspase-3 (rabbit monoclonal, 1:500, catalog no. 9961, Cell Signaling), insulin (Beta Cell Biology Consortium), or actin (mouse monoclonal, 1:500, ab3280, Abcam). Percentages of TUNEL-positive nuclei and insulin, cleaved caspase-3, or TUNEL double positive β-cells per islet were calculated and reported as means ± S.E., and the *p* values calculated using two-way analysis of variance followed by Bonferroni multiple comparison test post hoc analysis.

RESULTS

Vitamin A Deprivation Reduces Pancreatic Retinol Levels—We previously demonstrated that dietary VA deprivation in $LRAT^{-/-}$ mice rapidly results in major reductions in pancreatic retinoids (12), making $LRAT^{-/-}$ mice an ideal model to examine the role of VA in adult pancreatic biology. In this study we used both WT and $LRAT^{-/-}$ mice, a genetically modified model of impaired VA storage (12, 17), to define the role of VA in the adult pancreas without any confounding effects of gestational VA deficiency. After 4 weeks of VA deprivation, WT and $LRAT^{-/-}$ mice showed 17 and 81% reductions, respectively, in pancreatic ROL levels compared with WT and $LRAT^{-/-}$ mice

on a VAS diet (Fig. 1, *B* and *C*). After 10 weeks of dietary VAD, ROL levels decreased by ~73% in pancreatic tissue of WT and were not detectable in LRAT$^{-/-}$ mice (Fig. 1*B*, WT 10wVAD, LRAT$^{-/-}$ 10wVAD mice). Resumption of a VADR diet for 8 weeks restored pancreatic ROL levels in WT and LRAT$^{-/-}$ mice to levels similar to those in WT 10wVAS and LRAT$^{-/-}$ VAS mice (Fig. 1, *B* and *C*). Thus, we conclude that dietary VA deprivation decreases pancreatic ROL levels, which decline further with longer dietary VA deprivation. Because the LRAT$^{-/-}$ mice cannot store ROL in most tissues, their pancreatic ROL levels decrease more quickly than those in WT after VA removal from the diet (Fig. 1, *B* and *C*).

Dietary Vitamin A Deprivation in Adult Mice Leads to Impaired Glycemic and Insulin Responses—Because dietary VA deprivation leads to a striking decrease in pancreatic VA levels, we next assessed whether our 4- and 10-week dietary VA deprivation protocols caused alterations in glucose tolerance and glucose-stimulated insulin secretion. We performed GTT and found that in response to a glucose challenge LRAT$^{-/-}$ 4wVAD, LRAT$^{-/-}$ 10wVAD, and WT 10wVAD mice showed increased glucose excursions and area under the curve glucose, and reduced glucose-stimulated insulin secretion compared with VAS WT and LRAT$^{-/-}$ (Fig. 2, *A*, *B*, *D*, *E*, *G*, *H*, *J*, and *K*). Total pancreatic insulin content was reduced by 24% in LRAT$^{-/-}$ 4wVAD, 26% in WT 10wVAD, and 48% in LRAT$^{-/-}$ 10wVAD mice (Fig. 2, *F* and *L*). Islets from VAD WT and LRAT$^{-/-}$ mice also showed decreased insulin by immunohistochemistry (Fig. 2*M*). Using semiquantitative and real time PCR, we also detected relative reductions in pancreatic transcripts of pre-insulin genes (*ins1* and *ins2*) in pancreatic tissues from WT 10wVAD and LRAT$^{-/-}$ 10wVAD mice (Fig. 2*N*).

Gross histological analyses of islets from mice revealed that VA deprivation alters islet morphology, with islets from WT 10wVAD and LRAT$^{-/-}$ 10wVAD mice frequently showing irregularly shaped outlines and a lack of a discrete capsule compared with those from WT and LRAT$^{-/-}$ 10wVAS mice (Fig. 2*O*). Unlike pancreatic tissue, liver parenchyma (Fig. 2*O*) and kidney medullar and cortex regions (data not shown) from WT 10wVAD and LRAT$^{-/-}$ 10wVAD mice did not have evidence of altered tissue histology.

Peripheral insulin sensitivity was unaffected by VA deprivation (Fig. 2*P*), and random glucose (fed) levels were not different between WT 4wVAS and WT 4wVAD mice after 4 weeks of VA deprivation (Fig. 2*C*). However, we detected decreases in blood glucose levels in WT 10wVAD mice and, in contrast, elevations in blood glucose levels in LRAT$^{-/-}$ 10wVAD mice (Fig. 2*I*). These data suggest that VA deprivation results in a differential effect on random glucose regulation at this time point (Fig. 3, *F–I*), possibly because of the comparatively lower pancreatic VA levels of LRAT$^{-/-}$ 10wVAD compared with WT 10wVAD mice (Fig. 1*B*).

Resumption of dietary VA for 8 weeks normalized glucose excursions, insulin secretion responses, and pancreatic insulin content in WT and LRAT$^{-/-}$ VADR mice (Fig. 2, *G–L*). Islets of WT and LRAT$^{-/-}$ VADR mice showed increased insulin by immunohistochemistry, and mRNA levels of the pre-insulin genes *ins1* and *ins2* also increased (Fig. 2, *M* and *N*). Collectively, these data demonstrate that VA deprivation results in elevations in random glucose blood levels, impaired glucose-stimulated insulin secretion, and decreased pancreatic insulin content, but no alterations in peripheral insulin sensitivity.

Transcripts of Pancreatic Genes Involved in Retinoid Metabolism and Signaling Are Altered by VA Deprivation—The biologically active form of VA, all-*trans*-RA, can increase the transcript levels of some VA metabolizing proteins, such as Cyp26a1, and RA binding proteins, such as Crabp2 and RARβ2 (18–20). Thus, the relative mRNA levels of these and other RA-regulated genes can serve as a readout of the retinoid status and responsiveness of tissue. We performed quantitative real time PCR on whole pancreatic tissue instead of in isolated pancreatic islets because enzymatic and mechanical purification has been shown to alter the transcriptional profiles of islets (21, 22). Quantitative RT-PCR analysis of pancreatic tissues from VAD and VADR mice showed that pancreatic *RARα* and retinoid X receptor (*RXR*) α transcript levels were unaffected in the VAD WT and LRAT$^{-/-}$ compared with VAS WT and LRAT$^{-/-}$ mice (Fig. 3, *A* and *D*). In contrast, *RARβ2* and *RARγ2* transcript levels were greatly reduced in pancreata of VAD WT and LRAT$^{-/-}$ mice (Fig. 3, *B* and *C*). However, *RARα*, *RXRα*, *RARβ2*, and RARγ2 transcript levels were similar in VADR WT and LRAT$^{-/-}$ and in VAS WT and LRAT$^{-/-}$ (Fig. 3, *A–D*).

Dietary VA deprivation also resulted in reductions in pancreatic transcript levels of major intracellular retinoid carrier proteins, including *Crbp1*, *Crabp1*, and *Crabp2* (Fig. 3, *E–G*), and in transcript levels of *Cyp26a1* (Fig. 3*H*), the enzyme responsible for catabolism of RA (18). Relative transcript levels of *RARβ2*, *RARγ2*, *Crbp1*, *Crabp1*, *Crabp2*, and *Cyp26a1* in WT and LRAT$^{-/-}$ VADR mice, however, were similar to the levels in WT and LRAT$^{-/-}$ VAS mice (Fig. 3, *E–H*). These data demonstrate that dietary VA deprivation, reductions in pancreatic VA levels, and the subsequent metabolic phenotype caused by VA deprivation coincide with greatly reduced pancreatic transcript levels of genes involved in VA signal transduction, including *Crbp1*, *Crabp2*, *RARβ2*, *RARγ2*, and *Cyp26a1*. Thus, pancreatic retinoid signaling is impaired because of dietary VA deprivation.

VA Deprivation Decreases Crbp1 and Cyp26a1 Expression in Larger Islets—Crbp1 (also referred to as RBP1) is one of two major ROL cytoplasmic transport proteins, and Cyp26a1 is responsible for the metabolism of RA into polar metabolites (21, 22). Both are essential for normal VA metabolic and signaling homeostasis (23–25); therefore, given the reductions in Crbp1 and Cyp26a1 transcripts in VA-deprived mice (Fig. 3, *E* and *H*), we used double immunofluorescence microscopy to determine whether immunoreactivity to antibodies against Crbp1 and Cyp26a1 was reduced in islets of VAD mice.

We also sought to determine whether Crbp1 or Cyp26a1 is preferentially expressed in the endocrine or exocrine pancreas and whether patterns of Crbp1 and Cyp26a1 protein expression differ in large (30,000–20,000 μm^2), medium (20,000–10,000 μm^2), and small (10,000–2,000 μm^2) sized islets. We discovered that Crbp1 immunopositive cells are present within both the islets and exocrine acini (*white arrows*) of WT 10wVAS and LRAT$^{-/-}$ 10wVAS mice (Fig. 4, *A* and *D*); however, none of the Crbp1-positive islet cells was double positive for the β-cell

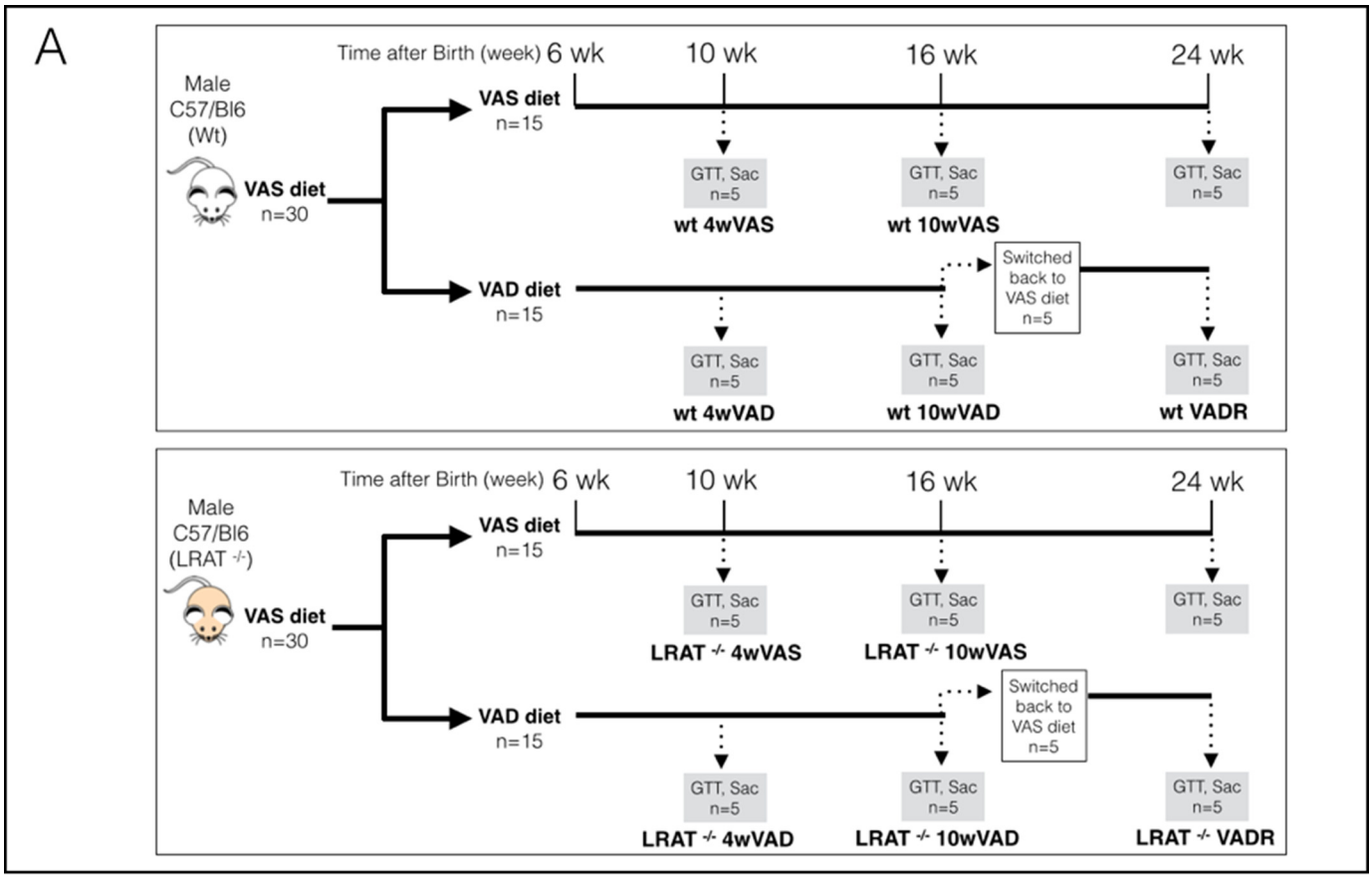
A
Time after Birth (week) 6 wk 10 wk 16 wk 24 wk
Male C57/Bl6 (Wt)
VAS diet n=30
VAS diet n=15
VAD diet n=15
GTT, Sac n=5
wt 4wVAS
wt 10wVAS
Switched back to VAS diet n=5
wt 4wVAD
wt 10wVAD
wt VADR
Male C57/Bl6 (LRAT -/-)
LRAT -/- 4wVAS
LRAT -/- 10wVAS
LRAT -/- 4wVAD
LRAT -/- 10wVAD
LRAT -/- VADR

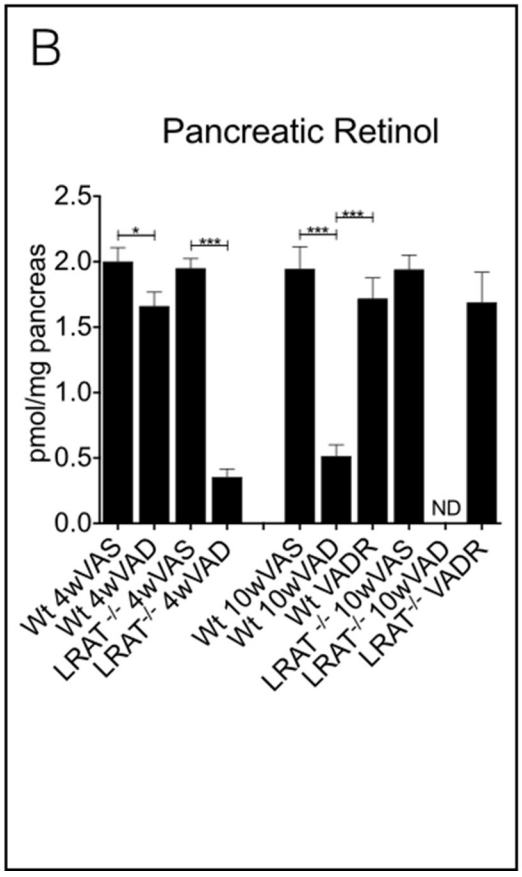
B
Pancreatic Retinol
pmol/mg pancreas
2.5
2.0
1.5
1.0
0.5
0.0
*
***
***
***
ND
Wt 4wVAS
Wt 4wVAD
LRAT -/- 4wVAS
LRAT -/- 4wVAD
Wt 10wVAS
Wt 10wVAD
Wt VADR
LRAT -/- 10wVAS
LRAT -/- 10wVAD
LRAT -/- VADR

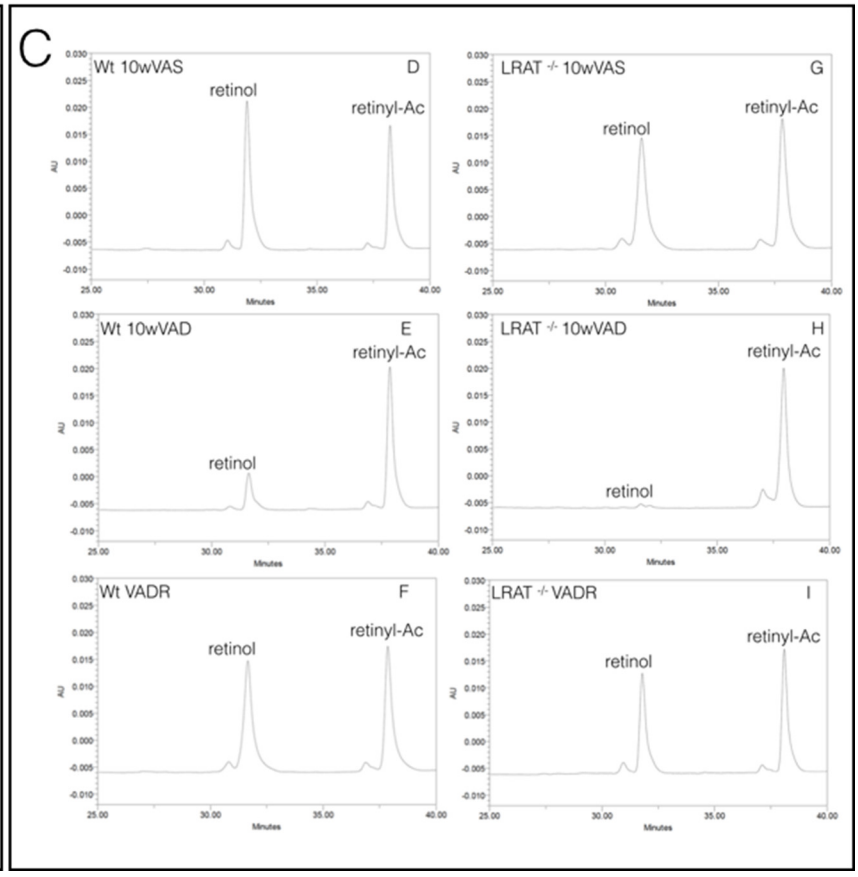
C
Wt 10wVAS
D
retinol
retinyl-Ac
LRAT -/- 10wVAS
G
Wt 10wVAD
E
LRAT -/- 10wVAD
H
Wt VADR
F
LRAT -/- VADR
I
AU
Minutes

marker C-peptide (Fig. 4, *A* and *D*, *white box* enlarged in *D*) or the α-cell marker glucagon (not shown). We did not detect Crbp1 immunopositive areas in ductal epithelial regions (Fig. 4, *A* and *D*).

Stellate cells are one of the principal VA storing cells in mammals and are found in numerous tissue types, including the pancreas (26). We performed double immunofluorescence staining of pancreatic sections with the stellate cell marker vimentin and Crbp1 antibodies to determine whether the Crbp1-positive cells are pancreatic stellate cells (PSCs). We found that more than 90% of the Crbp1-positive cells in the exocrine pancreas (Fig. 5*A* and *B*, *merged image*, *white arrows*) and islets (Fig. 5, *A* and *B*, *merged image*, *white arrows*) are positive for vimentin, and VA deprivation resulted in a 45–55% decrease in Crbp1-positive PSCs (Fig. 5*B*). We did not detect a decrease in the number of PSCs, nor did we detect an increase in PSC expression of α-smooth muscle actin (α-SMA) (not shown), a marker for activated PSCs, which confers loss of VA storage capacity (27). The decrease in the percentages of Crbp1-positive PSCs in VA-deprived mice prompted us to measure the pattern of Crbp1 expression across all islet sizes in VAS and VAD mice using direct morphometric analysis coupled to immunofluorescence staining.

Regression analysis demonstrated that islet expression of Crbp1 positively correlates with islet size in WT 10wVAS and LRAT$^{-/-}$ 10wVAS ($r = 0.85$, $r = 0.913$; Fig. 4*H*, *panels a* and *d*). This correlation is lost in pancreatic tissue of VA-deprived WT 10wVAD and LRAT$^{-/-}$ 10wVAD mice ($r = 0.256$, $r = 0.312$; Fig. 4*H*, *panels b* and *e*) as a result of the 80–90% aggregate decrease in Crbp1 protein in large and medium islets (Fig. 4*G*). VA deprivation did not decrease Crbp1 protein levels in the smallest islet pools (10,000–2,000 μm^2; Fig. 4*G*). Dietary VA rescue for 8 weeks, which restored pancreatic ROL levels (Fig. 1*B*), also restored the positive relationship between Crbp1 expression and islet size in WT VADR and LRAT$^{-/-}$ VADR mice ($r = 0.813$, $r = 0.712$; Fig. 4*H*, *c* and *f*). VA deprivation also led to a 3–5-fold reduction in exocrine pancreatic Crbp1-positive areas in WT 10wVAD and LRAT$^{-/-}$ 10wVAD mice (Fig. 4, *B*, *E*, and *G* (*VAD*), whereas exocrine pancreatic Crbp1-positive areas were again detected by 8 weeks after resumption of the VAS diet (Fig. 4, *C*, *F*, and *G* (*VADR*)).

The cytochrome P-450 enzyme Cyp26a1 mRNA and protein levels are strongly induced by RA (22), and Cyp26a1 levels are a key indicator of intracellular RA levels (22). We found that, similar to the expression pattern of Crbp1, both exocrine acini and islets (*white arrows*) were strongly immunopositive for Cyp26a1 (Fig. 4, *I* and *L*). Islet immunopositive Cyp26a1 cells did not express markers for pancreatic β-cells (Fig. 4*L*, *white box* enlarged) but as expected did express the stellate cell marker vimentin (not shown), supporting the notion that Cyp26a1-positive cells are PSCs. Cyp26a1 protein level is also positively correlated with islet size in WT and LRAT$^{-/-}$ 10wVAS (Fig. 4*P*, *a* and *d*), but not in WT 10wVAD and LRAT$^{-/-}$ 10wVAD mice (Fig. 4, *J*, *M*, and *P*, *panels b* and *e*) because of the 88–90% decrease in Cyp26a1 protein levels in the large to medium islet pools in both WT 10wVAD and LRAT$^{-/-}$ 10wVAD mice (Fig. 4*O*). The positive correlation between islet size and Cyp26a1 protein level was restored in both WT and LRAT$^{-/-}$ by 8 weeks of refeeding a VAS diet (Fig. 4, *K*, *N*, and *P*, *panels c* and *f* (*VADR*)).

Dietary Vitamin A Deprivation Leads to β-Cell Apoptosis in Large Islets—Given that retinoids possess the capacity to regulate apoptosis in vertebrates (28), we next determined whether removal of dietary VA caused changes in pancreatic programmed cell death. We coupled TUNEL staining with islet morphometric analyses to determine the percentages of apoptosis in large (30,000–20,000 μm^2), medium (20,000–10,000 μm^2), and small islets (10,000–1,000 μm^2) of 4 and 10 week VAS and VAD WT and LRAT$^{-/-}$ mice. We found no evidence of apoptosis in the exocrine or endocrine pancreata of mice fed the VAS diet (Fig. 6*A*, *panels a–c* and *j–l*, and *B*). Consistent with our data that LRAT$^{-/-}$ mice become VAD more rapidly than WT (12), we detected apoptosis in 60% of the cells in the large to medium sized islets and in 10% of the cells in the smaller islets in LRAT$^{-/-}$ 4wVAD mice, but we only detected apoptosis in ~1.5–2.5% of the cells in the large to medium islets and no apoptosis in the smaller islets of WT 4wVAD mice (Fig. 6*B*). WT 10wVAD and LRAT$^{-/-}$ 10wVAD mice showed disproportionately higher apoptosis in large to medium islets (~20–30%; *yellow arrowheads* in Fig. 6, *A*, *panels d*, *e*, *m*, and *n*, and *B*), compared with the small islets (~5%; *yellow arrowheads* in Fig. 6*A*, *panels f* and *o*, and *B*). Pancreatic islets from WT VADR mice exhibited apoptosis in only ~10% of the cells in the large and medium islets (*yellow arrowheads* in Fig. 6*A*, *panels g* and *h*, and *B*). LRAT$^{-/-}$ VADR mice showed no detectable apoptotic nuclei in large islets and apoptosis in only ~3–4% of the cells in the medium size islets (*yellow arrowheads* in Fig. 6, *A*, *panels p* and *q*, and *B*). In all conditions and in both WT and LRAT$^{-/-}$, the small islets showed less than 10% apoptosis (*yellow arrowheads* in Fig. 6, *A*, *panels c*, *f*, *i*, *l*, *o*, and r, and *B*).

Caspase-3 is a member of the family of cysteine proteases involved in executing early events in the apoptotic program (29). Proteolytic cleavage of caspase-3 marks the irreversible commitment of a cell to programmed cell death, a process that occurs before fragmentation of DNA (29). Given the decreased pancreatic insulin content of VA-deprived mice (Fig. 2, *J* and *L*),

FIGURE 1. *A*, dietary model of VA deficiency. 6–7-week-old WT and LRAT$^{-/-}$ male mice maintained on a lab chow diet (Pico Rodent Diet (#5053), Lab-Diets Co., St. Louis, MO) were switched to a VAS control diet (Harlan TD #88406, Madison, WI, [retinyl palmitate = 20 IU/gram]) for 1 week of acclimation and then randomly placed on the VAS diet or the VAD diet (Harlan #88407, Madison, WI; retinyl palmitate = 0.0 IU/gram) for 4 or 10 weeks. After 4 and 10 weeks, we subjected cohorts of mice on the VAS diet or VAD diet to GTT, sacrificed the mice, collected tissue and serum samples in the dark, and stored samples at −70 °C (4wVAS, 4wVAD, 10wVAS, and 10wVAD). At 10 weeks, additional cohorts of VA-deprived WT 10wVAD and LRAT$^{-/-}$ 10wVAD mice were switched back to a VAS diet (Harlan TD #88406, Madison, WI; retinyl palmitate = 20 IU/gram) for 8 weeks and were then subjected to GTT and sacrificed, and tissue and serum samples were collected and stored at −70 °C (VADR). Experiments were performed three times, starting with new groups of 6-week-old mice for each experiment ($n = 3$). *B*, HPLC analysis of all-*trans*-retinol in pancreata of VA-sufficient and -deprived mice. Quantitation of pancreatic retinol levels (pmol/mg pancreatic tissue) from WT and LRAT$^{-/-}$ mice subjected to 4 or 10 weeks of a VAS or VAD diet or 10 weeks of VAD diet followed by 8 weeks of VADR. *Errors bars* represent ± S.E. *, $p < 0.05$; ***, $p < 0.001$; *ND*, not detected. *C*, HPLC chromatograms of mice described for *A*. Based on retention times of pure standards, a single peak at 32.1 min was identified as all-*trans*-retinol, and a peak at 37.3 min was identified as retinyl acetate (*retinyl-Ac*) (internal standard).

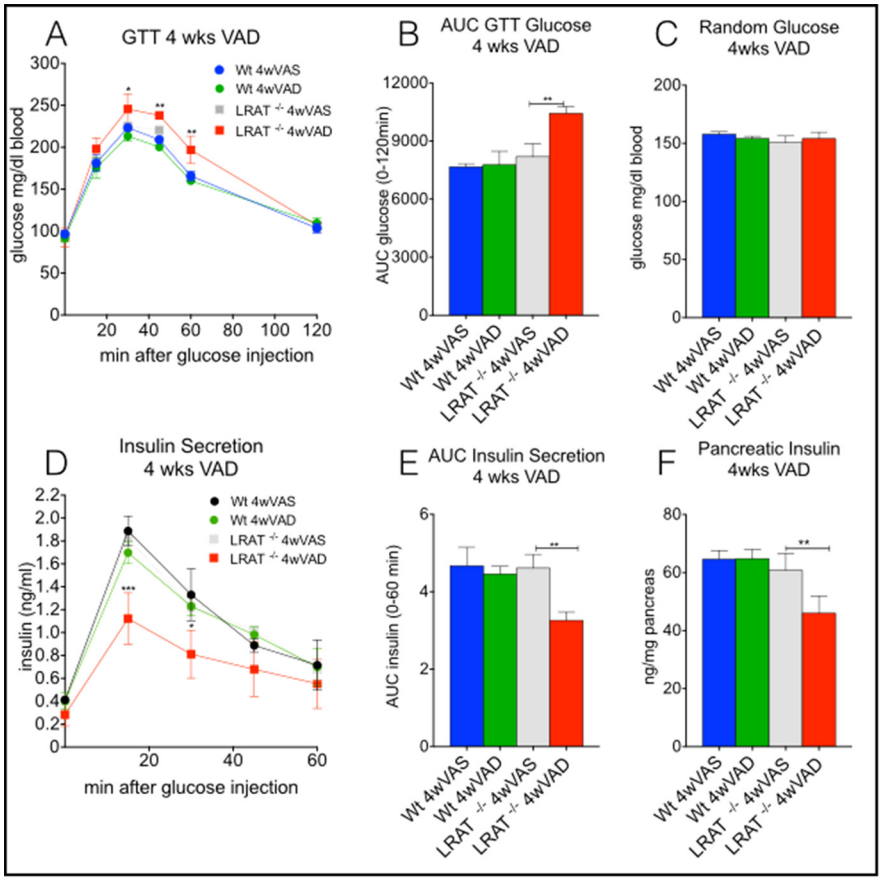
A
GTT 4 wks VAD
Wt 4wVAS
Wt 4wVAD
LRAT -/- 4wVAS
LRAT -/- 4wVAD
glucose mg/dl blood
min after glucose injection
B
AUC GTT Glucose
4 wks VAD
AUC glucose (0-120min)
C
Random Glucose
4wks VAD
glucose mg/dl blood
D
Insulin Secretion
4 wks VAD
insulin (ng/ml)
min after glucose injection
E
AUC Insulin Secretion
4 wks VAD
AUC insulin (0-60 min)
F
Pancreatic Insulin
4wks VAD
ng/mg pancreas
G
GTT 10 wks VAD
Wt 10wVAS
Wt 10wVAD
Wt VADR
LRAT -/- 10wVAS
LRAT -/- 10wVAD
LRAT -/- VADR
glucose mg/dl blood
min after glucose injection
H
AUC GTT Glucose
10 wks VAD
AUC glucose (0-120 min)
I
Random Glucose
10wks VAD
glucose mg/dl blood
J
Insulin Secretion
10 wks VAD
insulin ng/ml
min after glucose injection
K
AUC Insulin Secretion
10 wks VAD
AUC insulin (0-60 min)
L
Pancreatic Insulin
10 wks VAD
ng/mg pancreas

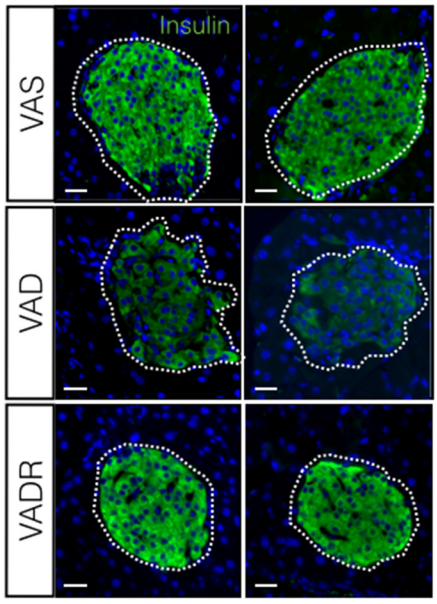
M
Insulin
VAS
VAD
VADR

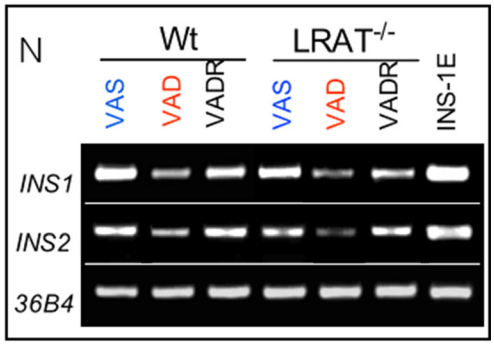
N
Wt
LRAT-/-
VAS
VAD
VADR
VAS
VAD
VADR
INS-1E
INS1
INS2
36B4

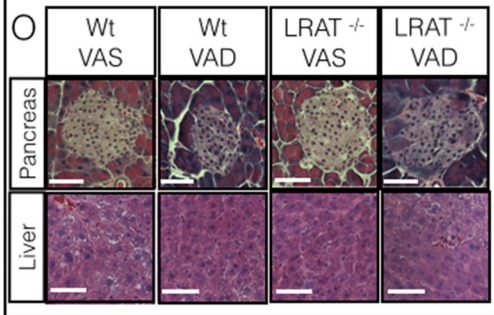
O
Wt
VAS
Wt
VAD
LRAT -/-
VAS
LRAT -/-
VAD
Pancreas
Liver

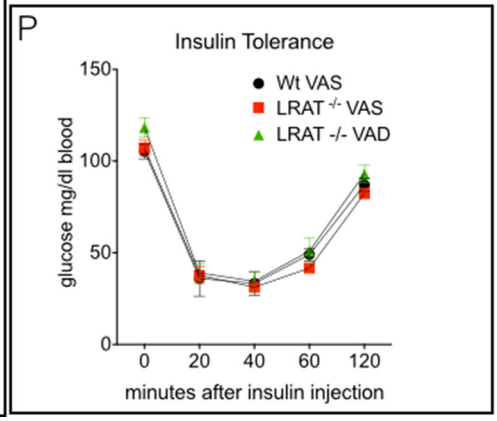
P
Insulin Tolerance
Wt VAS
LRAT -/- VAS
LRAT -/- VAD
glucose mg/dl blood
minutes after insulin injection

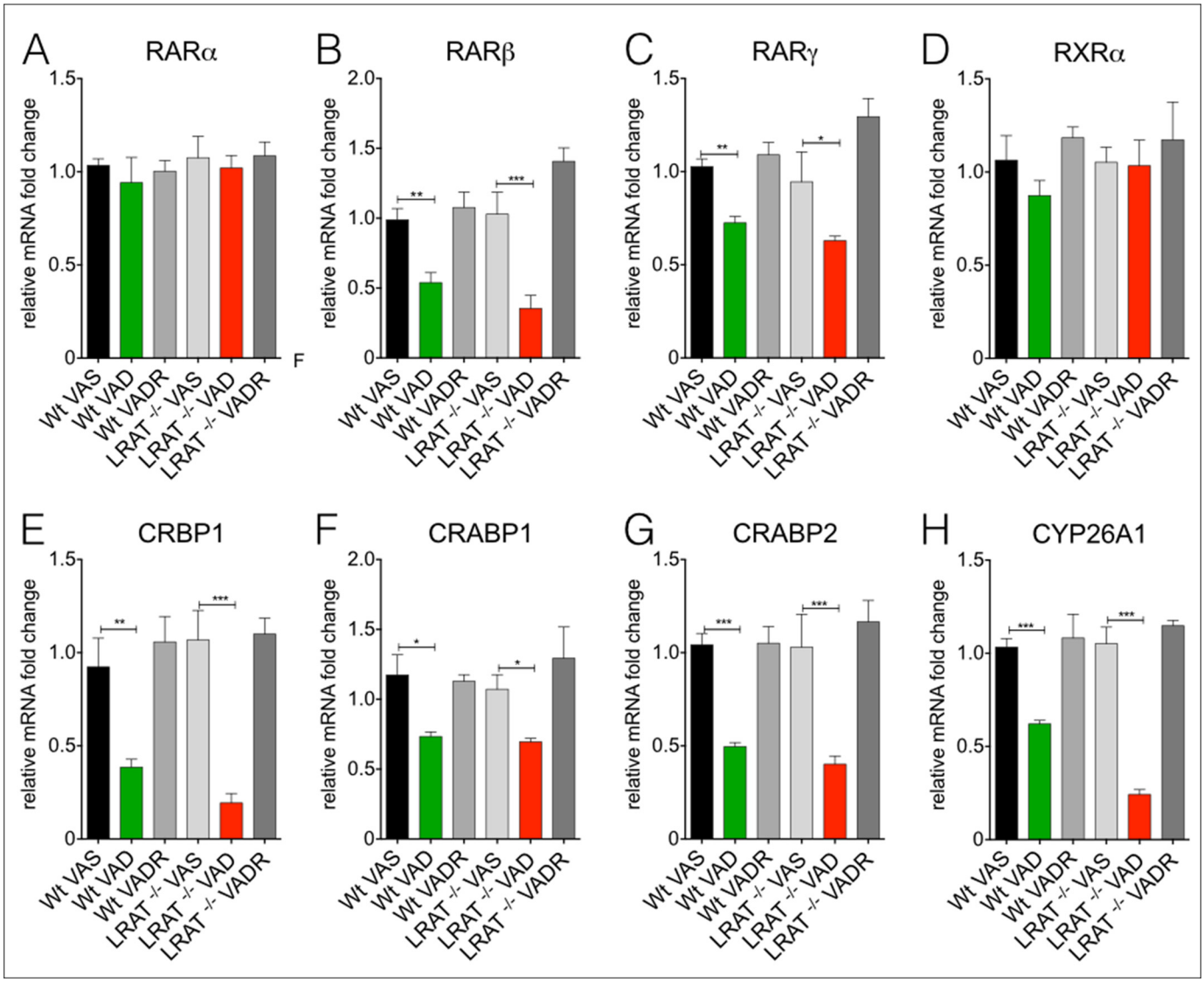

FIGURE 3. **Vitamin A deprivation alters pancreatic transcripts of retinoid signaling genes.** PCR measurements of relative pancreatic transcript levels of genes involved in RA signaling (*A–D*); VA and RA binding (*E–G*); and RA catabolism (*H*) were identified by quantitative real time PCR in WT and LRAT$^{-/-}$ 10wVAS, 10wVAD, or VADR mice. Relative fold mRNA levels were normalized to transcript levels of *Hprt* or *36b4*. *Errors bars* represent ± S.E. of (n = 5–6) animals per experimental group. *, $p < 0.05$; **, $p < 0.01$l; ***, $p < 0.001$.

we used double immunofluorescence staining of islets with antibodies against insulin (*green*) and cleaved caspase-3 (*red*) to determine whether pancreatic β-cells were the cells undergoing apoptosis in response to VA deprivation. Analysis of green channel (insulin) and red channel (cleaved caspase-3) merged immunofluorescence regions in large islet pools revealed the presence of numerous apoptotic β-cells in islets of VA-deprived WT and LRAT$^{-/-}$ mice (Fig. 6*C*, *upper panels*, *VAD*, *white arrowheads*, double-labeled, yellow/orange positive fields). WT 10wVAD and LRAT$^{-/-}$ 10wVAD mice showed 46 and 34% cleaved caspase-3-positive β-cells (Fig. 6*D*), which is consistent with the degree and pattern of TUNEL-positive islets in WT 10wVAD *versus* LRAT$^{-/-}$ 10wVAD mice (Fig. 6, *A* and *B*). Double immunofluorescence staining with cleaved caspase-3 and glucagon showed that less than 2% of α-cells were cleaved caspase-3 double positive in all experimental

FIGURE 2. **Dietary VA deprivation alters glycemic and insulin responses.** Serum glucose, area under the curve (*AUC*) glucose, insulin secretion, area under the curve insulin measurements during GTT, fed (random glucose), and pancreatic insulin levels in WT and LRAT$^{-/-}$ mice subjected to 4 weeks (*A–F*) of a VAS or VAD diet, 10 weeks (*G–L*) of a VAS or VAD diet, or 10 weeks of a VAD diet followed by 8 weeks of a VAS diet (VADR). *Errors bars* represent ± S.E. p values with *asterisks* are comparisons with WT VAS: *, $p < 0.05$; **, $p < 0.01$; ***, $p < 0.001$; ****, $p < 0.0001$. p values with plus signs are comparisons with LRAT$^{-/-}$ VAS: ++, $p < 0.01$; +++, $p < 0.001$; ++++, $p < 0.0001$. *M*, representative immunofluorescence images of pancreatic islet sections from WT and LRAT$^{-/-}$ mice subjected to 10 weeks of a VAS or VAD diet stained with mouse monoclonal antibody against insulin (*green*, 1:500). Magnification, 400×, *Scale bars*, 25 μm. *N*, representative images of ethidium bromide stained PCR products for genes *ins1* and *ins2* from pancreatic extracts from WT and LRAT$^{-/-}$ 10wVAS, 10wVAD, and VADR mice, or INS-1E cells (rodent β-cell line) as a positive control. *O*, representative hematoxylin- and eosin-stained pancreatic islet sections, and liver sections from WT and LRAT$^{-/-}$ 10wVAS and 10wVAD samples, Magnification, 400×; *Scale bars*, 100 μm. *P*, glucose levels in response to insulin tolerance testing in WT (n = 3) and LRAT$^{-/-}$ mice (n = 3) subjected to 8 weeks of VAS diet, and LRAT$^{-/-}$ mice (n = 3) subjected to 8 weeks of a VAD diet. *Errors bars* represent ± S.E.

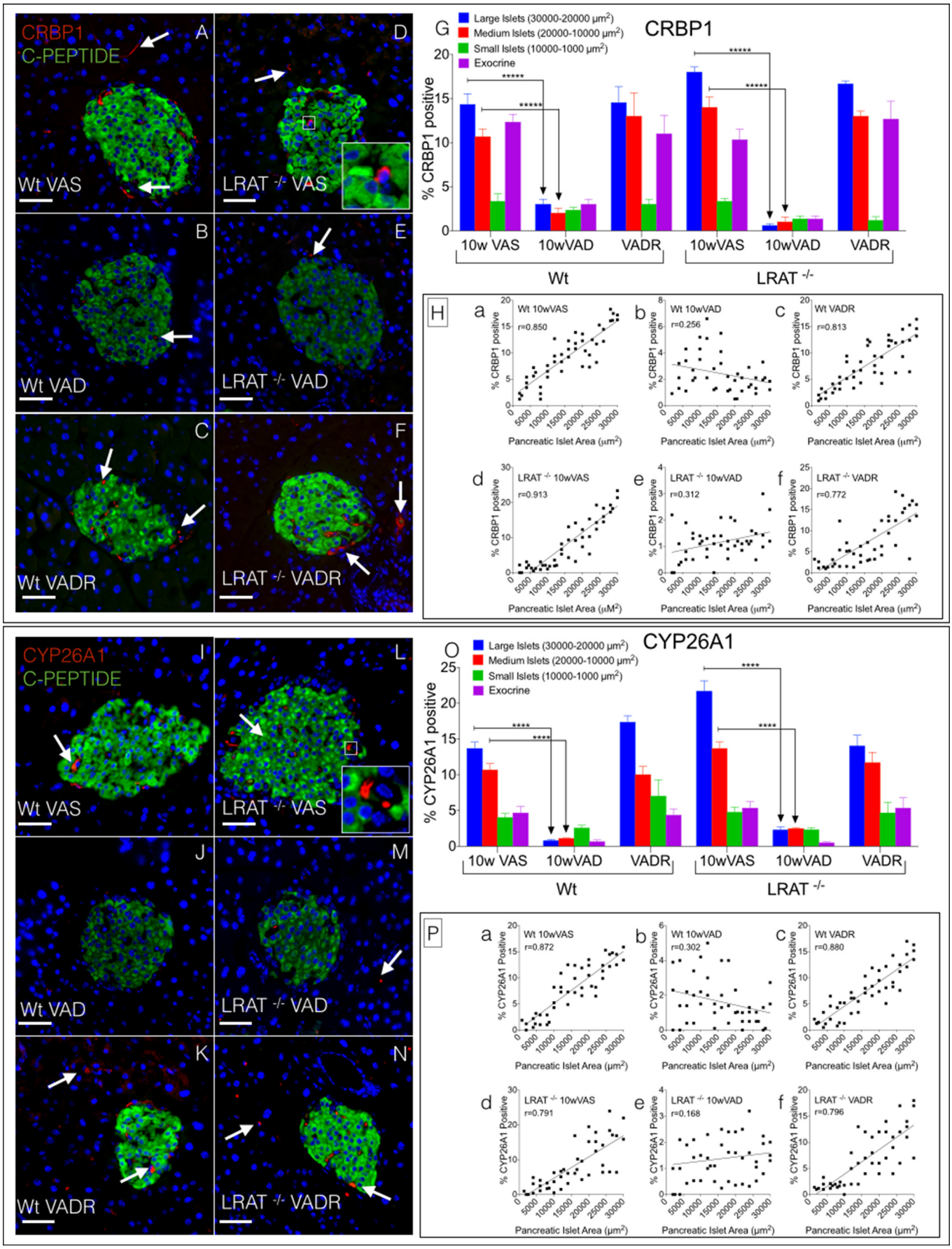
CRBP1
C-PEPTIDE
A
Wt VAS
D
LRAT -/- VAS
B
Wt VAD
E
LRAT -/- VAD
C
Wt VADR
F
LRAT -/- VADR
G
Large Islets (30000-20000 μm²)
Medium Islets (20000-10000 μm²)
Small Islets (10000-1000 μm²)
Exocrine
CRBP1
% CRBP1 positive
10w VAS
10wVAD
VADR
10wVAS
10wVAD
VADR
Wt
LRAT -/-
H
a Wt 10wVAS r=0.850
b Wt 10wVAD r=0.256
c Wt VADR r=0.813
d LRAT -/- 10wVAS r=0.913
e LRAT -/- 10wVAD r=0.312
f LRAT -/- VADR r=0.772
Pancreatic Islet Area (μm²)
CYP26A1
C-PEPTIDE
I
Wt VAS
L
LRAT -/- VAS
J
Wt VAD
M
LRAT -/- VAD
K
Wt VADR
N
LRAT -/- VADR
O
Large Islets (30000-20000 μm²)
Medium Islets (20000-10000 μm²)
Small Islets (10000-1000 μm²)
Exocrine
CYP26A1
% CYP26A1 positive
10w VAS
10wVAD
VADR
10wVAS
10wVAD
VADR
Wt
LRAT -/-
P
a Wt 10wVAS r=0.872
b Wt 10wVAD r=0.302
c Wt VADR r=0.880
d LRAT -/- 10wVAS r=0.791
e LRAT -/- 10wVAD r=0.168
f LRAT -/- VADR r=0.796
Pancreatic Islet Area (μm²)

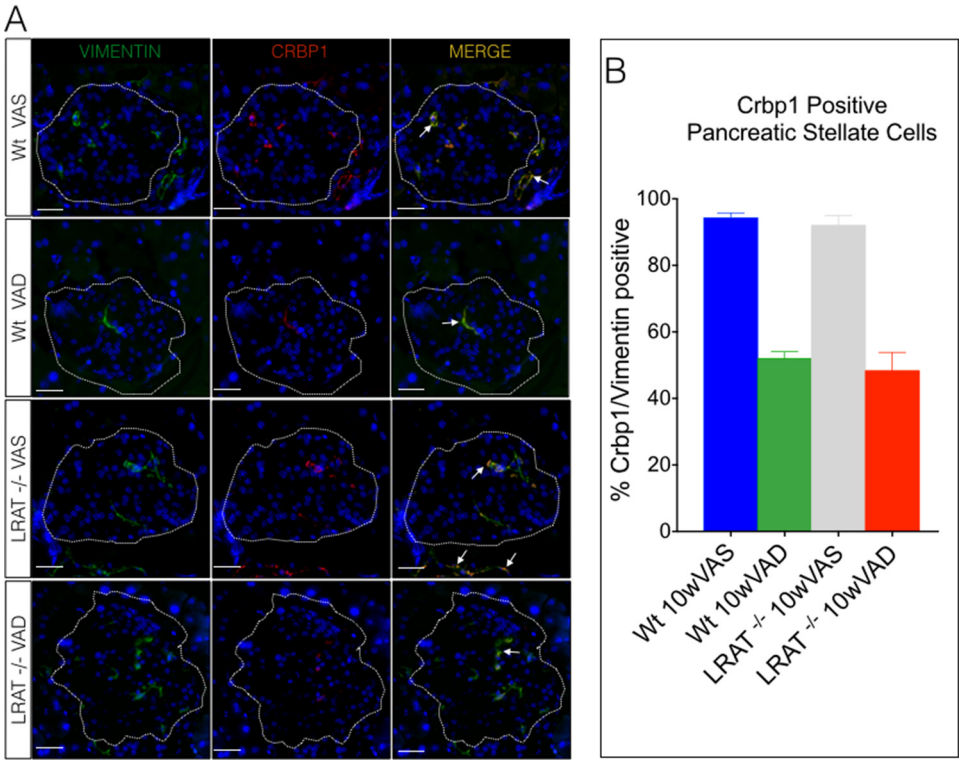

FIGURE 5. **Crbp1-positive cells are pancreatic stellate cells.** *A*, representative images of pancreatic sections double immunofluorescence stained with antibodies against vimentin (*green*) and Crbp1 (*red*) from WT and LRAT$^{-/-}$ 10wVAS and 10wVAD mice. Magnification, 400×; *scale bars*, 100 μm. *B*, quantitation of percentage of Crbp1-positive pancreatic stellate cells in mice described for *A*. *Errors bars* represent mean percentages of vimentin and Crbp1 double positive cells ± S.E. of $n = 4–5$ mice per group.

groups (data not shown). We also performed double TUNEL and insulin staining of islets to determine whether the percentage of caspase-3-positive β-cells is an indicator of the percentage of β-cells that undergo apoptosis in response to VA deprivation. We found that, consistent with our caspase-3 staining and colorimetric TUNEL assays, VA deprivation leads to ~30–40% β-cell apoptosis (*lower panels*, *white arrows*, blue/green nuclei; Fig. 6, *C* and *D*).

To determine whether VA-deprived mice experienced broad, nonspecific programmed cell death in various other tissues we performed TUNEL staining of frozen liver, kidney, and small intestine sections from WT and LRAT$^{-/-}$ VAS and VAD mice and found no increase in apoptosis associated with VA deprivation in these tissues (not shown). Importantly, these data indicate that although we induced dietary VAD in the entire animals, the pancreas β-cells are uniquely sensitive to VAD compared with other cell types in the various other organs.

Dietary Vitamin A Deprivation Reduces Pancreatic Islet Sizes but Not Islet Numbers—Given the marked increase in islet apoptosis that we observed in WT 10wVAD, LRAT$^{-/-}$ 4wVAD, and LRAT$^{-/-}$ 10wVAD mice, coupled with the absence of compensatory endocrine cell proliferation in VA rescued mice, we hypothesized that apoptosis in larger islets would diminish the mean islet area of VA-deprived mice. We first comprehensively measured pancreatic islet size distributions by direct morphometric analysis of 4 and 10 weeks VAS WT and LRAT$^{-/-}$ mice, which exhibit a leftward skewed pattern of islet size distributions consistent with what has been reported in mice, humans, and other vertebrates using direct morphometric and mathematical model analyses (Fig. 7, *A–D*) (30–32). LRAT$^{-/-}$ 4wVAD showed a 38% decrease of large to medium sized islets (30,000–16,000 μm^2) and a concomitant 34% increase in medium to small sized islets (16,000–4,000 μm^2), but no change in the smallest islet populations (200–4,000 μm^2) compared with LRAT$^{-/-}$ 4wVAS mice (Fig. 7*B*). No relative changes in islet size distributions were detected in WT 4wVAD mice (Fig. 7*A*). We detected additional changes in islet size distributions in both WT 10wVAD and LRAT$^{-/-}$ 10wVAD mice, including a 92–97% reduction in large islets (30,000–20,000 μm^2), a 70–85% reduction in medium size islets (20,000–10,000 μm^2), and a 38–40% increase in the smallest islets (10,000–200 μm^2) (Fig. 7, *C* and *D*).

FIGURE 4. **Vitamin A status affects pancreatic expression of Crbp1 and Cyp26a1.** *A–F*, representative images of pancreatic islets, double immunofluorescence stained with antibodies against Crbp1 and C-peptide from WT and LRAT$^{-/-}$ 10wVAS, 10wVAD, and VADR mice. Magnification, 400×; *scale bars*, 100 μm. *G*, quantitation of percentage Crbp1-positive areas of large islets (30,000–20,000 μm^2), medium islets (20,000–10,000 μm^2), and small islets (10,000–2,000 μm^2) of mice described for *A–F*. *Error bars* represent ± S.E. *****, $p < 0.00001$. *H*, *panels a–f*, correlation between percentage Crbp1-positive islets and islet areas from mice described for *A–F*. *I–N*, representative images of pancreatic islets, double immunofluorescence stained with antibodies against Cyp26a1 and C-peptide from mice described for *A–F*. *Magnification*, 400×; *scale bars*, 100 μm. *O*, quantitation of percentage Cyp26a1-positive areas of large islets (30,000–20,000 μm^2), medium islets (20,000–10,000 μm^2), and small islets (10,000–2,000 μm^2) of mice described for *A–F*. *Errors bars* represent ± S.E. *****, $p < 0.00001$. *P*, *panels a–f*, correlation between percentage of Cyp26a1-positive islets and islet areas from mice described for *A–F* (for all panels, $n = 3$).

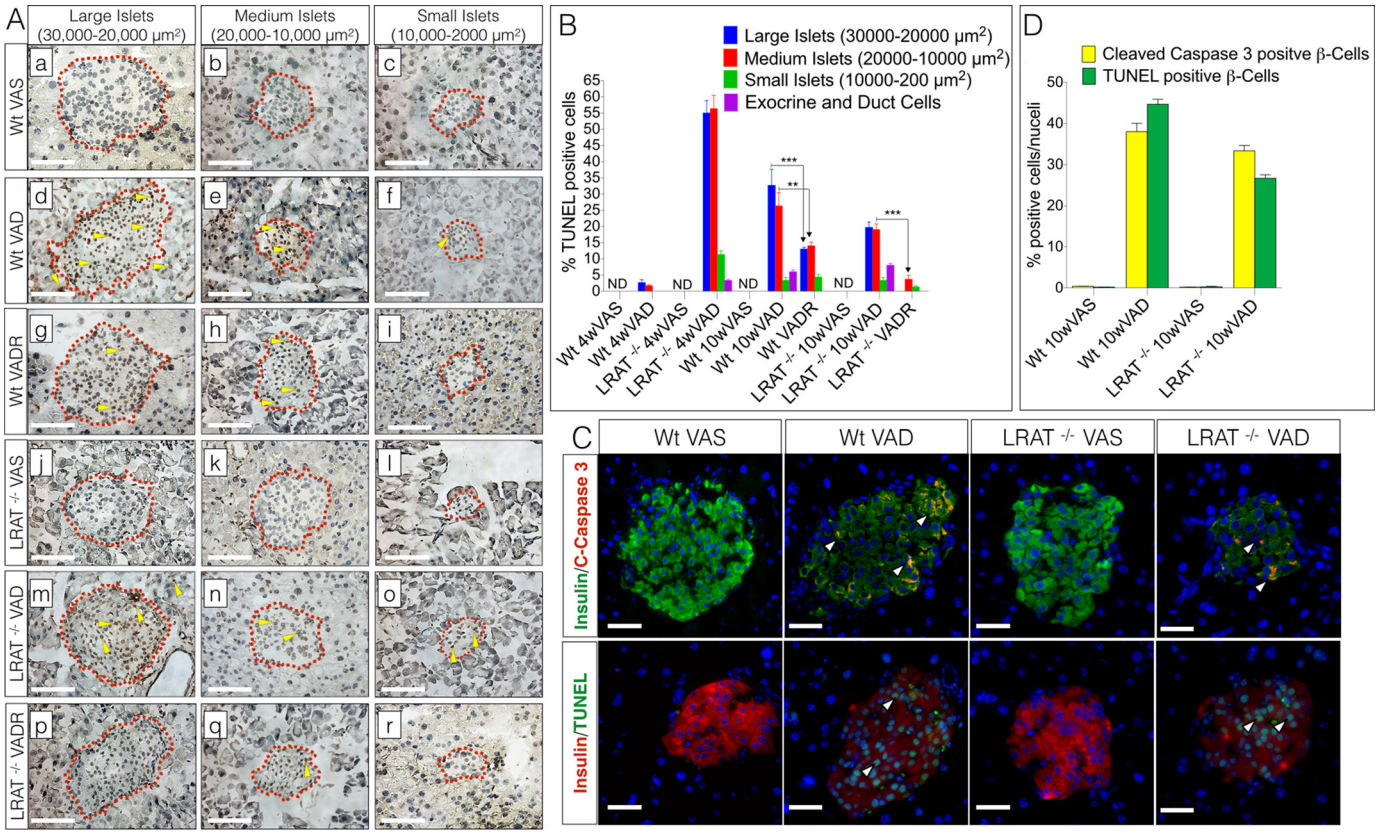

FIGURE 6. **Increased apoptosis in VA-deprived mice.** *A*, *panels a–r*, representative images of TUNEL stained pancreatic islets of WT and LRAT$^{-/-}$ 10wVAS, 10wVAD, and VADR mice. Magnification, 200×; *scale bars*, 100 μm. *B*, quantitation of percentages of islet positive TUNEL cells in WT and LRAT$^{-/-}$ 4wVAS, 4wVAD, 10wVAS, 10wVAD, and VADR mice. *Error bars* represent ± S.E. **, $p < 0.01$; ***, $p < 0.001$. *C*, *upper panels*, representative images of pancreatic islets double immunofluorescence stained with insulin (*green*) and caspase-3 (*red*) from WT and LRAT$^{-/-}$ 10wVAS and 10wVAD mice. Double positive cleaved caspase-3 (*red*) and insulin (*green*) fields (*yellow*/*orange*) are indicated with *white arrows*. Magnification, 400×; *scale bars*, 100 μm. *C*, *lower panels*, representative images of pancreatic islets double immunofluorescence stained with TUNEL (*green*) and insulin (*red*) from mice described for *C*. Nuclei (*blue*/DAPI) of TUNEL-positive, apoptotic β-cells fluoresce *green*/*blue* and are indicated with *white arrows*. Magnification, 400×; *scale bars*, 100 μm. *D*, quantitation of pancreatic β-cells cell apoptosis from samples in *C*. *Errors bars* represent ± S.E. of $n = 4–5$ mice per group.

Dietary VA deprivation did not alter the total number of islets, pancreatic weights, or body weights of WT or LRAT$^{-/-}$ mice (Fig. 7, *E*, *G*, and *H*), which consequently resulted in significant reductions in mean pancreatic islet areas that coincided with the frequent appearances of clusters of smaller islet pools in both WT 10wVAD and LRAT$^{-/-}$ 10wVAD mice compared with VAS WT and LRAT$^{-/-}$ mice (Fig. 7, *F*, *I*, *J*, *L*, and *M*). Pancreatic islet size distributions in VA rescued WT VADR and LRAT$^{-/-}$ VADR mice were similar to those in WT 10wVAS and LRAT$^{-/-}$ 10wVAS mice (Figs. 7*C* and 6*D*), and the presence of smaller islet clusters was not observed in pancreatic sections of WT VADR and LRAT$^{-/-}$ VADR mice (Fig. 7, *K* and *N*). We conclude that VAD causes a dynamic leftward shift in the pancreatic islet size distributions.

Vitamin A Deprivation Causes a Decrease in β-Cell Mass—We next determined whether VA deprivation affected endocrine cell mass, given the decreases in pancreatic β-cells (Fig. 6*C*) and mean islet areas of VA-deprived WT and LRAT$^{-/-}$ mice (Fig. 7*F*). Our analysis demonstrated that WT 4wVAD mice had no evidence of diminished endocrine cell mass (Fig. 8, *A* and *B*). However, consistent with the reduced pancreatic insulin levels (Fig. 2*F*) and glucose-stimulated insulin secretion (Fig. 2*D*) observed after 4 weeks of VA deprivation, LRAT$^{-/-}$ 4wVAD mice had a 37% ($p < 0.001$) decrease in β-cell mass (Fig. 8*A*, *black bars*). Interestingly, we also detected a 48% ($p < 0.001$) reduction in α-cell mass (Fig. 8*B*, *black bars*), and 28 and 30% reductions in serum insulin and glucagon, respectively, compared with LRAT$^{-/-}$ 4wVAS mice (Fig. 8, *D* and *E*). These analyses support the thesis that our genetic model of impaired VA storage, LRAT$^{-/-}$ mice, display both hormonal and pancreatic endocrine changes in response to VA deprivation much earlier than VA-deprived WT mice. Although WT 10wVAD mice begin to display the same reductions in glucose-stimulated insulin and pancreatic insulin content observed in VA-deprived LRAT$^{-/-}$ mice (Fig. 2, *G* and *J*), LRAT$^{-/-}$ 10wVAD mice showed more severe reductions in pancreatic VA levels (Fig. 1*B*), glucose-stimulated insulin secretion, and pancreatic insulin content compared with WT 10wVAD mice (Fig. 2, *G*, *J*, and *L*). Consistent with this, our β-cell mass measurements demonstrate that both LRAT$^{-/-}$ 10wVAD and WT 10wVAD mice display large reductions in β-cell mass (77 and 38%) and serum insulin (60 and 30%) compared with VAS LRAT$^{-/-}$ and WT mice, respectively (Fig. 8, *A*, *D*, and *G*, panels *a–f* and *j–o*); however, both the β-cell mass profile and serum insulin level of LRAT$^{-/-}$ 10wVAD mice were ~50% lower than WT 10wVAD mice (Fig. 8, *A* and *D*).

Next we analyzed α-cell mass and found a more varied pattern of α-cell mass measurements between LRAT$^{-/-}$ 10wVAD

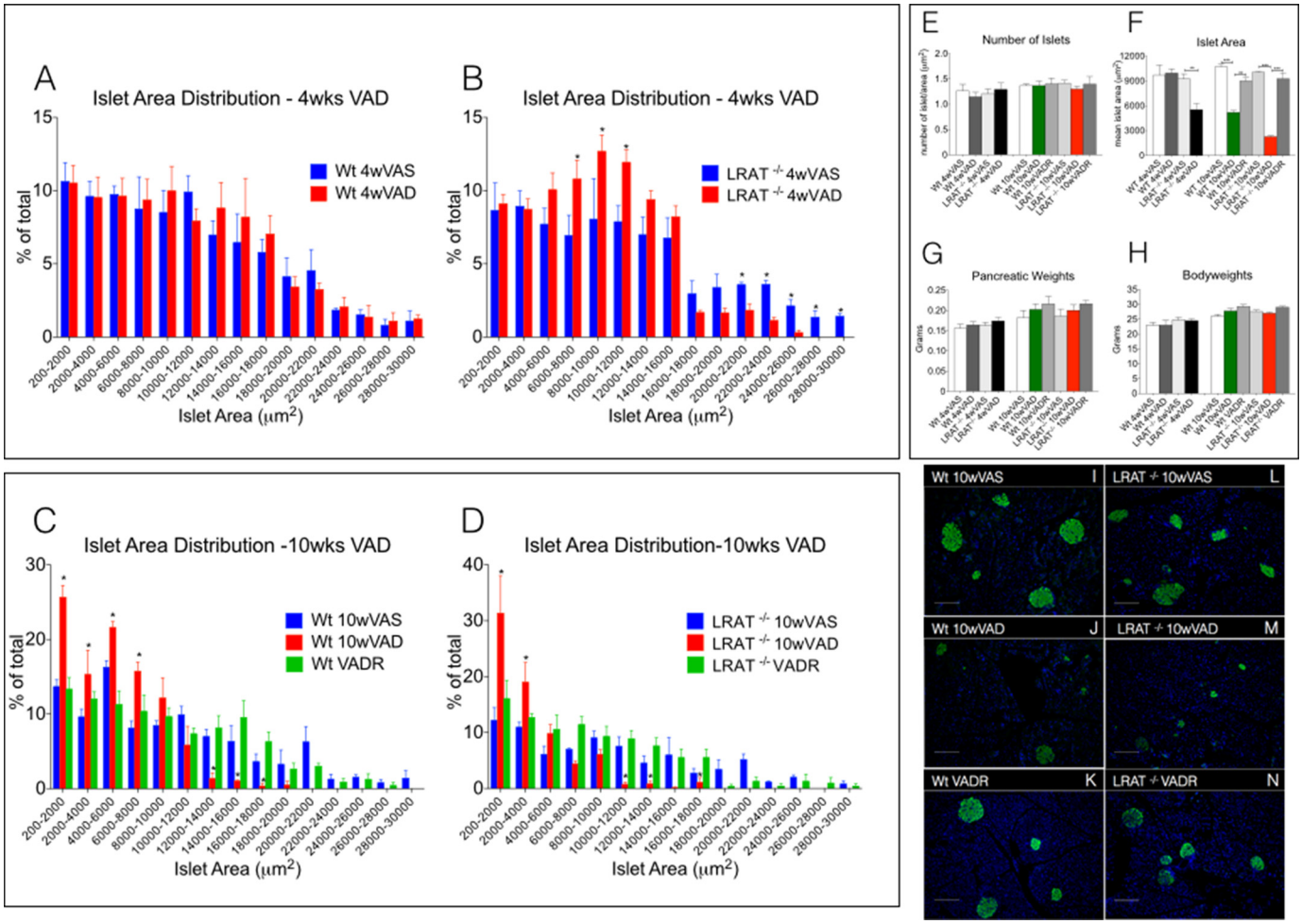

FIGURE 7. **Altered pancreatic islet distributions in VA-deprived mice.** *A–D*, relative percentages of large islets (30,000 –20,000 μm^2), medium islets (20,000 – 10,000 μm^2), and small islets (10,000 –200 μm^2) in WT and LRAT$^{-/-}$ 4wVAS AND 4wVAD mice (*A* and *B*) or 10wVAS, 10wVAD, or VADR mice (*C* and *D*). *E*, mean islet numbers per unit area (μm^2) of pancreata from mice described for *A–D*. *F*, mean body weights of mice in *A–D*. *G*, mean pancreatic weights of mice described for *A–D*. *H*, mean islet area per unit area (μm^2) of pancreata from mice described for *A–D*. *Errors bars* represent ± S.E. *, $p < 0.05$; **, $p < 0.01$; ***, $p < 0.001$. *I–N*, representative images of insulin-stained pancreatic islets of mice described for *C* and *D*. Magnification, 100×; *scale bars*, 25 μm.

and WT 10wVAD mice. LRAT$^{-/-}$ 10wVAD mice showed a 67% ($p < 0.001$) increase in pancreatic α-cell mass, whereas, in stark contrast, WT 10wVAD mice showed a 67% ($p < 0.001$) reduction in α-cell mass compared with WT 10wVAS mice (Fig. 8*B*). Pancreatic (Fig. 8*F*) and serum glucagon (Fig. 8*E*) levels reflected the α-cell mass profiles of both LRAT$^{-/-}$ 10wVAD and WT 10wVAD mice. LRAT$^{-/-}$ 10wVAD mice also exhibited a marked increase in α-cells (*red*, glucagon positive) in the islet centers (Fig. 8*G*, panels *m–o*); this was also observed to a lesser degree in WT 10wVAD (Fig. 8*G*, *panels d–f*) compared with the WT and LRAT$^{-/-}$ 10wVAS mice (Fig. 8*G*, *a–c* and *j–l*).

The increase in pancreatic α-cell to β-cell mass ratios and the resultant hyperglucagonemia of LRAT$^{-/-}$ 10wVAD mice (Fig. 8, *C*, *E*, and *F*) were reflected in their elevated fasting glucose levels (Fig. 8*H*) and increased hepatic transcripts levels of glycogen phosphorylase (*pygl*) (Fig. 8*I*) compared with LRAT$^{-/-}$ 10wVAS mice (Fig. 8, *H* and *I*). Also in agreement with their decreased circulating glucagon (Fig. 8*E*), fasting glucose levels (Fig. 8*H*) and hepatic transcripts of *pygl* (Fig. 8*I*) of WT 10wVAD mice were ~10% lower than the levels in WT 10wVAS mice (Fig. 8, *H* and *I*) and, accordingly, ~40% lower than the levels in LRAT$^{-/-}$ 10wVAD mice (Fig. 8, *H* and *I*).

Consistent with our observations that reintroducing dietary VA for 8 weeks reversed the impaired insulin secretion (Fig. 2*G*), low pancreatic insulin levels (Fig. 2, *L* and *M*), and low VA levels (Fig. 1*B*) in WT and LRAT$^{-/-}$ VADR mice, our analyses showed near reversal of α-cell to β-cell mass ratios (Fig. 8*C*), serum insulin (Fig. 7*D*), serum glucagon (Fig. 8*E*), fasting glucose levels (Fig. 8*H*), and islet architecture in both the WT and LRAT$^{-/-}$ 10wVADR mice (Fig. 8*G*, *panels g–i*, and *p–r*, respectively). These data also show that WT and LRAT$^{-/-}$ 10wVAD mice show differences in pancreatic endocrine cell and hormone profiles in response to VA deprivation that are related to the more rapid onset and greater severity of the decline in pancreatic VA levels in the LRAT$^{-/-}$ mice (Fig. 1*B*). These endocrine mass studies additionally reveal that alterations in endocrine cell profiles (*i.e.* α-cell to β-cell mass ratios) brought on by VA deprivation are not permanent and are reversible.

Modulation of Endocrine Cell Mass by Vitamin A Does Not Alter Markers of Proliferation or Neogenesis—Retinoids can increase the proliferation of endocrine cell progenitors and

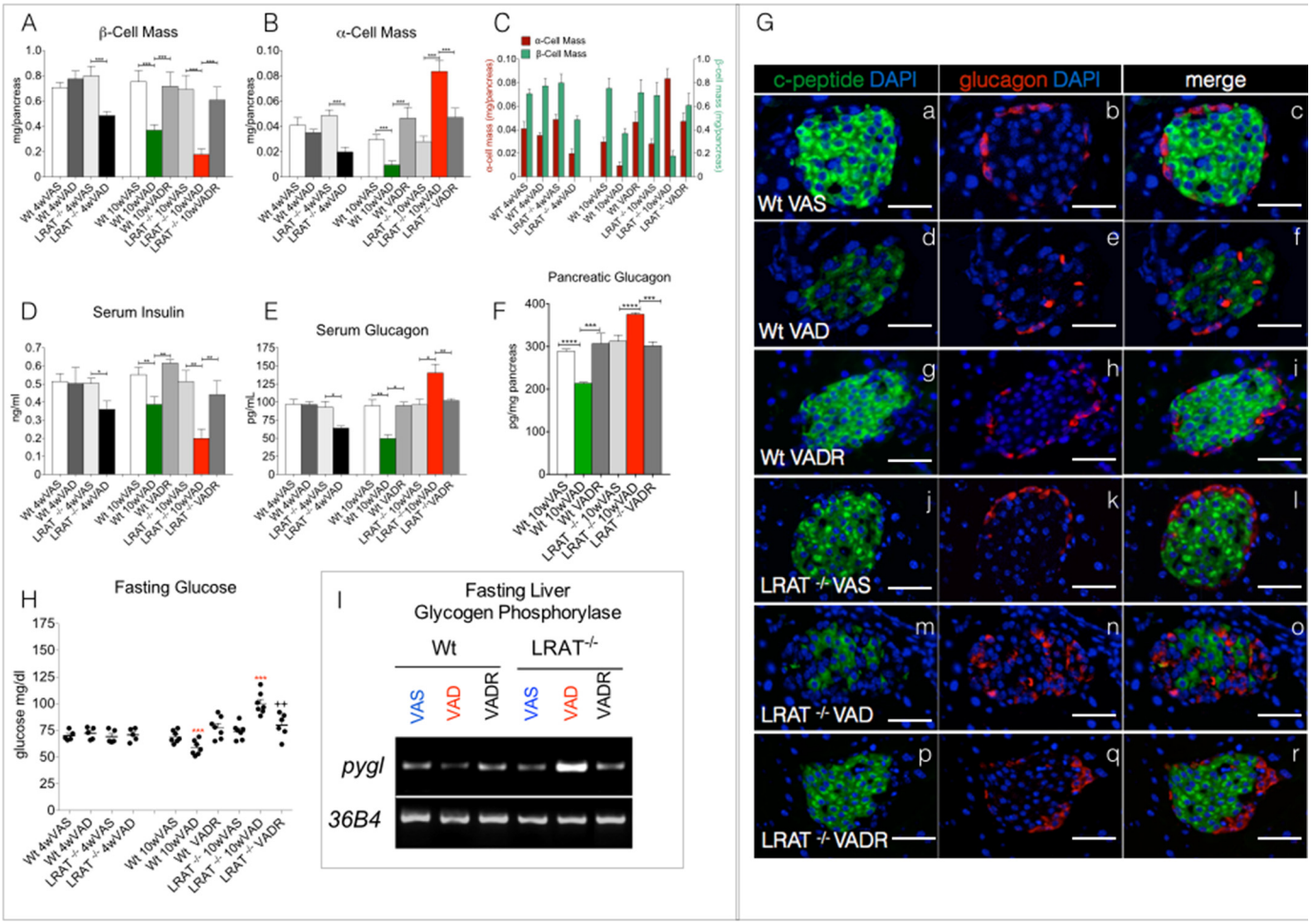

FIGURE 8. **Vitamin A deprivation alters pancreatic endocrine mass and hormones.** *A* and *B*, quantification of pancreatic β-cell and α-cell mass of WT and LRAT$^{-/-}$ 4wVAS, 4wVAD, 10wVAS, 10wVAD, and VADR mice. *C*, ratios of α-cell and β-cell mass from mice in A. ***, $p < 0.05$ *versus* LRAT$^{-/-}$ VAS. ++, $p < 0.01$ *versus* LRAT$^{-/-}$ VAD. *Errors bars* represent ± S.E. *, $p < 0.05$; **, $p < 0.01$; ***, $p < 0.001$. *D* and *E*, serum insulin and serum glucagon levels from mice described for *A*. *F*, pancreatic glucagon concentrations (pg/mg) from mice described for *A*. *G*, *panels a–r*, representative images of α-cells and β-cells from pancreatic islets of mice described for *A*. Magnification, 400×; *scale bars*, 100 μm. *H*, fasting blood glucose levels in mice described for *A*. *I*, semiquantitative PCR of hepatic mRNA transcripts of glycogen phosphorylase (*pygl*) from mice described for *A*, WT and LRAT$^{-/-}$ 10wVAS, 10wVAD, and VADR. ($n = 4$).

insulin-positive β-cells during pancreagenesis (5, 33), and there are data demonstrating that β-cell neogenesis can occur in response to β-cell ablation or pancreatic injury (34–36). Therefore, given that VA rescued mice had restored endocrine mass profiles in response to the reintroduction of dietary VA, we sought to determine whether the restoration of β-cell and α-cell mass in response to VA restoration was associated with increased proliferation of β-cells or other pancreatic cell types. Using monoclonal antibodies against Ki-67, proliferating cell nuclear antigen and insulin, we performed double immunofluorescence staining of pancreatic tissue to label actively proliferating β-cells. We found that the aggregate percentage of proliferating Ki-67-positive β-cells (*white arrows*, *purple nuclei* in Fig. 9, *A* and *B*) and nonendocrine cells (*yellow arrows*, purple nuclei in Fig. 9, *A* and *B*) was ~1.5–1.8% in WT and LRAT$^{-/-}$ 10wVAS samples and that this percentage was unchanged by VA deprivation or VA rescue (Fig. 9, *A* and *B*).

We then asked whether the restoration of β-cell mass in VADR mice was associated with changes in expression of two transcription factors: Ngn3 and pancreatic duodenal homeobox-1 (Pdx1). Ngn3 is required for development of all endocrine cell types during pancreagenesis (37), and in recent years data support the idea that pancreatic Ngn3-positive cells can repopulate the endocrine pancreas with newly generated β-cells in response to injury or toxin-induced destruction of β-cell mass (34, 38, 39). Pdx1 is another developmental transcription factor that is essential to development of insulin-producing β-cells (40). Pdx1 also has a role in β-cell regeneration and maturation of insulin secretory machinery and islet growth and expansion (41–43).

We used a monoclonal antibody to Ngn3 that can detect murine Ngn3-positive progenitors in models of pancreatic injury (44). Using a double immunofluorescence approach with antibodies against C-peptide and Ngn3, we were unable to detect endogenous Ngn3-positive areas in our analysis of more than 100 pancreatic endocrine cells, exocrine cells, and ductal fields in all of the dietary VA experimental groups (Fig. 9*C*, *panels a–f*).

We also analyzed pancreatic Pdx1 staining by immunohistochemistry and were able to detect Pdx1 immunopositive regions in the islets, acini (Fig. 9, *D*, *panels a* and *d*, and *E*), and pancreatic ductal regions (*red arrows* in Fig. 9, *D*, *panels a* and

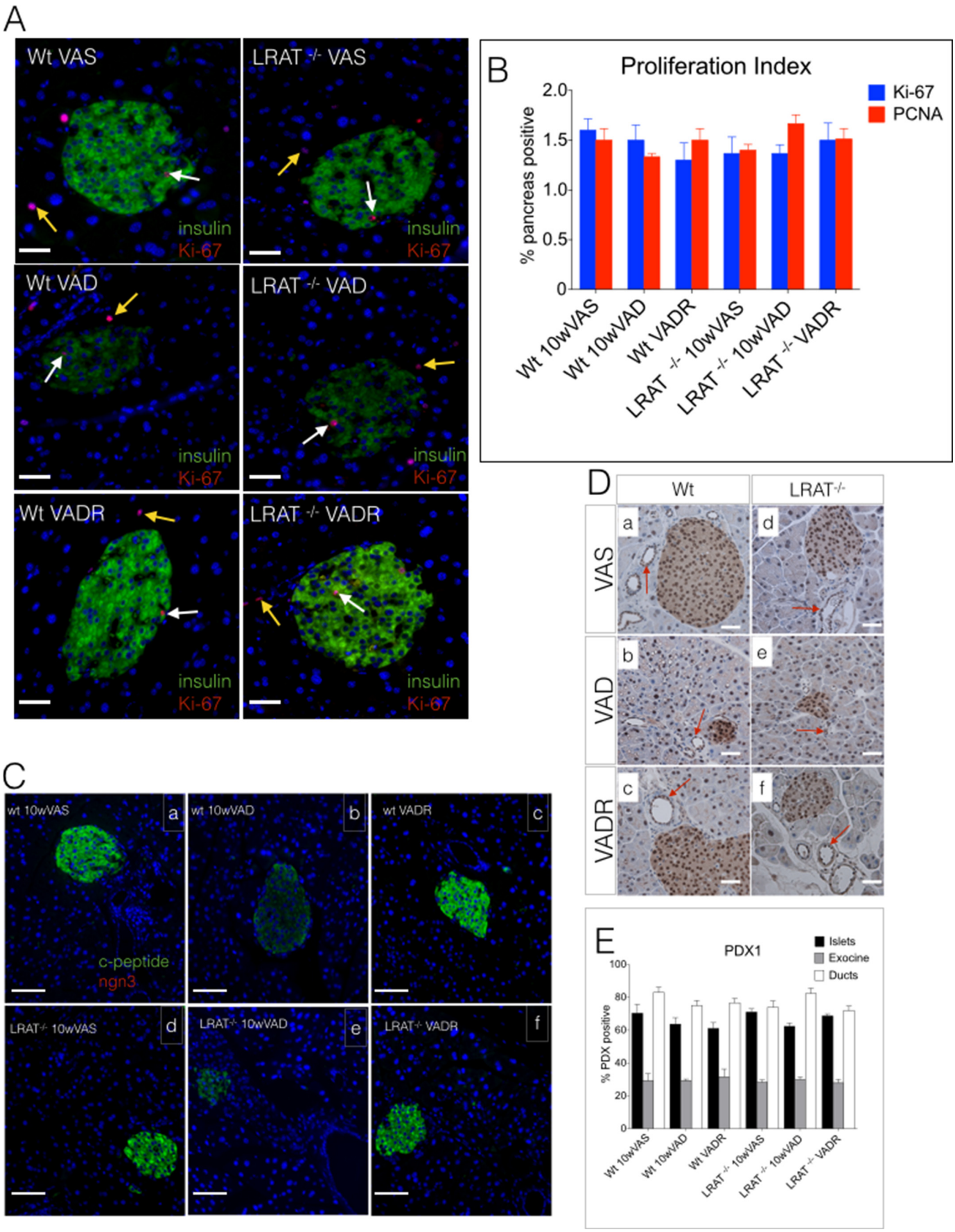
A
Wt VAS
LRAT -/- VAS
Wt VAD
LRAT -/- VAD
Wt VADR
LRAT -/- VADR
insulin
Ki-67
B
Proliferation Index
% pancreas positive
2.0
1.5
1.0
0.5
0
Ki-67
PCNA
Wt 10wVAS
Wt 10wVAD
Wt VADR
LRAT -/- 10wVAS
LRAT -/- 10wVAD
LRAT -/- VADR
C
wt 10wVAS
wt 10wVAD
wt VADR
c-peptide
ngn3
LRAT-/- 10wVAS
LRAT-/- 10wVAD
LRAT-/- VADR
D
Wt
LRAT-/-
VAS
VAD
VADR
E
PDX1
Islets
Exocine
Ducts
% PDX positive
100
80
60
40
20
0
Wt 10wVAS
Wt 10wVAD
Wt VADR
LRAT -/- 10wVAS
LRAT -/- 10wVAD
LRAT -/- VADR

d, and *E*) of WT and LRAT$^{-/-}$ 10wVAS mice. In our analysis of more than 100 pancreatic fields, we did not detect differences in pancreatic Pdx1 immunopositive ductal regions (*white arrows* in Fig. 9, *D*, *panels b*, *e*, *c*, and *f*, and *E*) or islets (Fig. 9*D*, *panels b*, *e*, *c*, and *f*, and *E*) in WT and LRAT$^{-/-}$ 10wVAD or in WT and LRAT$^{-/-}$ VADR mice. Collectively, these experiments demonstrate that VAD-mediated loss and VA-mediated restoration of pancreatic endocrine cell mass do not involve changes in pancreatic cell proliferation or neogenesis.

DISCUSSION

Numerous experimental studies have determined that VA and retinoids possess anti-obesity and anti-lipogenic properties through transcriptional regulation of relevant genes in liver and adipose tissue (45–47), but it is unclear whether altered VA metabolism is involved in the pathogenesis of T2D. There is a large body of data demonstrating that insulin resistance alters adipose and renal metabolism of RBP4 (retinol binding protein 4), which paradoxically further promotes insulin resistance and the pathogenesis of T2D (48, 49). Testament to the growing interest in retinoids as metabolic modulating agents is the recent initiation of phase 2 clinical trials of the synthetic retinoid fenretinide 4-hydroxy(phenyl)retinamide as a novel anti-obesity and insulin-sensitizing agent (50). Still, there remain large gaps in our knowledge of the mechanisms of 4-hydroxy-(phenyl)retinamide and retinoids in modulating the metabolic and endocrine pathways involved in the pathogenesis of obesity, insulin resistance, and T2D. To date, few studies have thoroughly examined the role of retinoids in pancreatic islet biology. In this study, we report that dietary VA is required for the maintenance of normal pancreatic islet architecture, endocrine cell mass, and endocrine function in adult, nondiabetic mice.

Our 4- and 10-week glucose tolerance tests, insulin secretion assays, and apoptosis studies show that as early as 4 weeks after the initiation of the VAD diet, the LRAT$^{-/-}$ mice had increased glucose excursions, decreased pancreatic insulin content, and marked (>50%) pancreatic islet apoptosis (Figs. 2, *A* and *F*, and 6*B*). By week 10 of VA deprivation, LRAT$^{-/-}$ 10wVAD mice displayed undetectable levels of pancreatic VA (Fig. 1*B*) and greatly diminished glucose-stimulated insulin secretion and pancreatic insulin content compared with LRAT$^{-/-}$ 10wVAS mice (Fig. 2, *G*, *J*, and *L*). Our apoptosis measurements in LRAT$^{-/-}$ mice also show that VA deprivation causes marked β-cell apoptosis (Fig. 6, *A–D*), a loss of β-cells (Fig. 8*A*), a major reduction in total pancreatic islet area (Fig. 7*F*), and, consequently, reduced basal insulin levels in the pancreas (Fig. 2, *F* and *L*). These experiments clearly demonstrate that with increasing severity of pancreatic VA depletion, the degree of impaired glucose tolerance correlates with the loss of β-cell mass.

The onset of a strikingly similar, but less severe, metabolic phenotype in WT 10wVAD mice compared with LRAT$^{-/-}$ 10w VAD mice provides further evidence that the earlier onset and increased relative severity of the glucose intolerance and pancreatic β-cell apoptosis we observed in VA-deprived LRAT$^{-/-}$ mice was not due to an unspecified metabolic anomaly related to their genotype but rather to their greater sensitivity to the lack of VA in the diet (12). Without any evidence of changes in peripheral insulin sensitivity (Fig. 2*P*), decreased body weights (Fig. 7*H*), or increased cell death and histological changes in other organs, such as the liver, kidney, and small intestines in the VAD mice, our data suggest that pancreatic endocrine functions and specifically the maintenance of β-cell populations are reliant on VA. However, given the complex interplay among pancreas, liver, adipose, and other tissues in regulating glucose homeostasis, we cannot exclude the possibility that VA deprivation alters metabolic pathways in other tissues that contribute to the pancreatic endocrine phenotype of VA-deprived and rescued mice.

Our Crbp1 and Cyp26a1 islet immunostaining studies provide evidence for how the pancreas senses changes in tissue retinoid levels and how large islets are specifically affected by decreases in pancreatic VA levels. Decreased cellular Crbp1 and Cyp26a1 levels are associated with poor retinoid responsiveness and low cellular RA levels (23, 25). We show that when dietary and pancreatic VA levels are sufficient, expression of both Crbp1 and Cyp26a1 correlates with islet size, but that this is not the case under dietary VA deprivation (Fig. 4, *H*, *panels a*, *b*, *d*, and *e*, and *P*, *panels a*, *b*, *d*, and *e*). Additionally, the reductions and subsequent restoration of pancreatic *Crbp1*, *Cyp26a1*, *RARβ2*, and *RARγ2* transcripts in WT and LRAT$^{-/-}$ VAD *versus* VADR mice, respectively (Fig. 3), are compelling and support our hypothesis that VA deprivation reduces pancreatic VA levels that are critical for retinoid signaling and normal pancreatic control of glucose-stimulated insulin release in the adult pancreas. Thus, we interpret the reductions in Crbp1 and Cyp26a1, as assessed by our immunostaining studies (Fig. 4), that occur in concert with the reductions in pancreatic VA levels (Fig. 1*B*) to indicate that dietary VA deprivation prevents the growth and proper functioning of pancreatic islets. That the large islets with the highest percentages of Crbp1 and Cyp26a1 immunopositive regions are preferentially targeted for apoptosis (Fig. 6*C*) and remodeling during VA deprivation (Fig. 6, *A–D*) suggests that a reduction in Crbp1 and Cyp26a1 expression provides pancreatic cells an early cue of diminishing VA availability and, if VA levels continue to drop, leads to an intrinsic cascade of β-cell programmed cell death and islet remodeling.

FIGURE 9. **VA deprivation or refeeding does not alter pancreatic cell proliferation or expression of ngn3 or Pdx1.** *A*, representative images of pancreatic islets double immunofluorescence stained with antibodies against insulin (*green*) and Ki-67 (*red*) in WT and LRAT$^{-/-}$ mice subjected to 10 weeks of a VAS or VAD diet or 10 weeks of VAD diet followed by 8 weeks of a VAS diet (VADR). Magnification, 400×; *scale bars*, 100 μm. *B*, quantitation of percentage of positive pancreatic endocrine and exocrine cells for antibodies against Ki-67 and proliferating cell nuclear antigen (*PCNA*; images not shown). *C*, *panels a–f*, representative images of pancreatic sections double immunofluorescence stained with antibodies against Ngn3 and C-peptide (*green*) from 5–7 mice per group described for *A*. Magnification, 200×; *scale bars*, 150 μm. *D*, *panels a–f*, representative images of Pdx1-positive pancreatic sections from mice described for *A*. *Red arrows* indicate Pdx1-positive ductal regions. Magnification, 200×; *scale bars*, 50 μm. *E*, quantitation of percentage of Pdx1-positive pancreatic islets, exocrine, and ductal areas of mice described for *A*. *Errors bars* represent mean percentages of Pdx1-positive cells ± S.E. of $n = 4–5$ mice per group.

Lepr^{db}, C57BLKS mice, commonly refereed to as "db/db" mice, are a commonly used genetic model for advanced T2D (51). With age and progression of the diabetic phenotype, db/db mice exhibit a similar pancreatic islet phenotype as VAD mice, with marked β-cell apoptosis, reduced insulin levels, and larger islets (31, 52). Evidence suggests that humans with T2D also experience a specific loss of larger islet pools (53, 54).

The loss of larger islet pools was dynamic in that it occurred with a concomitant increase in the percentage of smaller islet sizes (Fig. 7, *A–D*). This islet remodeling is more suggestive of a concerted metabolic response to VA deprivation rather than broad, nonspecific cell death. The absence of increased apoptosis in liver, kidney, and small intestines of VA-deprived mice supports this notion and demonstrates that the pancreatic β-cells are more sensitive to reductions in dietary and pancreatic VA than other cell types in these other organs. The absence of any changes in total islet numbers (Fig. 7*E*), pancreatic weights (Fig. 7*G*), endocrine cell proliferation, and markers of β-cell neogenesis (Fig. 9, *A*, *C*, and *D*) during VA deprivation provides strong evidence that the increased numbers of medium to small islets in WT 10wVAD and LRAT$^{-/-}$ 10wVAD mice (Fig. 7, *A–D*) are derived from apoptosis in previously larger islets and not from proliferation of pancreatic progenitors. The lack of islet apoptosis (Fig. 6, *A* and *B*) and the normalization of islet size distributions (Fig. 7, *C* and *D*) in the VA-deprived mice after restoration of dietary VA also support the notion of a specific, nonpermanent, reversible metabolic program in response to VA deprivation. We conclude that β-cell apoptosis and loss of islet mass do not result from nonspecific glucotoxicity secondary to VA deprivation, because WT VA-deprived mice are hypoglycemic, and LRAT$^{-/-}$ VAD mice show only marginal hyperglycemia (Fig. 8*H*). Moreover, we did not detect histopathology hallmarks of pancreatic glucotoxicity such pancreatitis, islet amyloid deposits, and fibrosis (55). Therefore, one mechanism by which mice remodel islet size is through modulation of pancreatic VA signaling and apoptosis.

We also found that VA deprivation results in aberrations in endocrine cell mass profiles. By week 10 of VA deprivation, both WT 10wVAD and LRAT$^{-/-}$ 10wVAD mice showed losses of β-cell mass (Fig. 8*A*) and decreased fasting serum insulin levels (Fig. 8*D*). Interestingly, LRAT$^{-/-}$ 10wVAD mice showed elevated α-cell mass, pancreatic glucagon, and glucagon serum concentrations compared with WT 10wVAS and LRAT$^{-/-}$ 10wVAS mice (Fig. 8). The elevated glucose profile and increased hepatic expression of glycogen phosphorylase also suggest that the hyperglucagonemia in LRAT$^{-/-}$ 10wVAD mice results in increased hepatic mobilization of glycogen stores and is responsible for the increased fasting hyperglycemia in these LRAT$^{-/-}$ mice. It is unclear whether the increased number of α-cells is secondary to the loss of β-cell mass. The degree of β-cell apoptosis, the increased α-cell mass, and the presence of α-cells within islet centers of LRAT$^{-/-}$ 10wVAD mice (Fig. 8, *B*, *red bar*, and *G*, *panels m–o*) are consistent with increased numbers and the presence of hyper-responsive, glucagon-secreting α-cells within the islets in experimental diabetic rodent models involving β-cell ablation (56–58). In contrast, WT 10wVAD mice showed a decrease in α-cell mass, pancreatic and serum hypoglucagonemia, decreased fasting glucose levels, and increased intraislet α-cells (*white arrows* in Fig. 8*G*, *panels d–f*) as compared with WT VAS mice (Fig. 8, *B* and *E*). The dissimilar pancreatic endocrine cell and hormone profiles of WT and LRAT$^{-/-}$ 10w VA-deprived mice are likely a consequence of LRAT$^{-/-}$ mice showing the effects of VA deprivation earlier than WT mice. This is apparent from the earlier onset of apoptosis, glucose intolerance, and the severely diminished pancreatic VA levels observed in LRAT$^{-/-}$ mice, but not in WT mice, at 4 weeks of VA deprivation (Figs. 6*B*; 4, *A*, *B*, *D*, and *E*; and 1*B*). We predict that with continued VA deprivation, WT mice will develop hyperglucagonemia similar to that seen in the LRAT$^{-/-}$ 10wVAD mice.

We showed that the reduction in and subsequent restoration of pancreatic β-cell mass during VA deprivation and VA rescue, respectively, are not related to changes in β-cell proliferation or neogenesis from Ngn3-positive pancreatic progenitors (Fig. 9, *A–C*). Thus, we think that the restored β-cells in VA rescued WT and LRAT$^{-/-}$ VAD mice are derived from other endocrine cell types, given the evidence that endocrine cells can transdifferentiate into each other with ectopic expression of a number of developmental transcription factors, such as Pax 4 and ARX (59–61). Further experiments are required to determine whether VA can regulate the expression of these and other developmental transcription factors in the adult pancreas.

In summary, our data strongly demonstrate that VA plays a major role in maintaining the β-cell mass of larger sized islet populations. Mechanistically, we demonstrate that VA supports β-cells through prevention of programmed cell death. Alterations in pancreatic VA levels may be one method through which endocrine cell identities and islet plasticity are altered. Thus, we suggest that synthetic retinoids can be used in the future to prevent β-cell cell apoptosis in T2D.

Acknowledgments—We thank Dr. Xiao-Han Tang for assistance with HPLC and Dr. Jose Jessurun from the Department of Surgical Pathology at Weill Cornell Medical Center for evaluation of histology sections.

REFERENCES

1. Gudas, L. J., and Wagner, J. A. (2011) Retinoids regulate stem cell differentiation. *J. Cell. Physiol.* **226,** 322–330
2. Gudas, L. J. (2013) Retinoids induce stem cell differentiation via epigenetic changes. *Semin. Cell Dev. Biol.* **24,** 701–705
3. Martín, M., Gallego-Llamas, J., Ribes, V., Kedinger, M., Niederreither, K., Chambon, P., Dollé, P., and Gradwohl, G. (2005) Dorsal pancreas agenesis in retinoic acid-deficient Raldh2 mutant mice. *Dev. Biol.* **284,** 399–411
4. Molotkov, A., Molotkova, N., and Duester, G. (2005) Retinoic acid generated by Raldh2 in mesoderm is required for mouse dorsal endodermal pancreas development. *Dev. Dyn.* **232,** 950–957
5. Oström, M., Loffler, K. A., Edfalk, S., Selander, L., Dahl, U., Ricordi, C., Jeon, J., Correa-Medina, M., Diez, J., and Edlund, H. (2008) Retinoic acid promotes the generation of pancreatic endocrine progenitor cells and their further differentiation into beta-cells. *PLoS One* **3,** e2841
6. Kane, M. A., Folias, A. E., Pingitore, A., Perri, M., Obrochta, K. M., Krois, C. R., Cione, E., Ryu, J. Y., and Napoli, J. L. (2010) Identification of 9-*cis*-retinoic acid as a pancreas-specific autacoid that attenuates glucose-stimulated insulin secretion. *Proc. Natl. Acad. Sci. U.S.A.* **107,** 21884–21889
7. Pérez, R. J., Benoit, Y. D., and Gudas, L. J. (2013) Deletion of retinoic acid receptor β (RARβ) impairs pancreatic endocrine differentiation. *Exp. Cell*

Res. **319,** 2196–2204
8. Chertow, B. S., Blaner, W. S., Baranetsky, N. G., Sivitz, W. I., Cordle, M. B., Thompson, D., and Meda, P. (1987) Effects of vitamin A deficiency and repletion on rat insulin secretion in vivo and in vitro from isolated islets. *J. Clin. Invest.* **79,** 163–169
9. Chertow, B. S., Driscoll, H. K., Blaner, W. S., Meda, P., Cordle, M. B., and Matthews, K. A. (1994) Effects of vitamin A deficiency and repletion on rat glucagon secretion. *Pancreas* **9,** 475–484
10. Matthews, K. A., Rhoten, W. B., Driscoll, H. K., and Chertow, B. S. (2004) Vitamin A deficiency impairs fetal islet development and causes subsequent glucose intolerance in adult rats. *J. Nutr.* **134,** 1958–1963
11. Donath, M. Y., and Halban, P. A. (2004) Decreased beta-cell mass in diabetes: significance, mechanisms and therapeutic implications. *Diabetologia* **47,** 581–589
12. Liu, L., and Gudas, L. J. (2005) Disruption of the lecithin:retinol acyltransferase gene makes mice more susceptible to vitamin A deficiency. *J. Biol. Chem.* **280,** 40226–40234
13. Guo, L., Inada, A., Aguayo-Mazzucato, C., Hollister-Lock, J., Fujitani, Y., Weir, G. C., Wright, C. V., Sharma, A., and Bonner-Weir, S. (2013) PDX1 in ducts is not required for postnatal formation of β-cells but is necessary for their subsequent maturation. *Diabetes* **62,** 3459–3468
14. Suh, J. M., Jonker, J. W., Ahmadian, M., Goetz, R., Lackey, D., Osborn, O., Huang, Z., Liu, W., Yoshihara, E., van Dijk, T. H., Havinga, R., Fan, W., Yin, Y. Q., Yu, R. T., Liddle, C., Atkins, A. R., Olefsky, J. M., Mohammadi, M., Downes, M., and Evans, R. M. (2014) Endocrinization of FGF1 produces a neomorphic and potent insulin sensitizer. *Nature* **513,** 436–439
15. Pfaffl, M. W. (2001) A new mathematical model for relative quantification in real-time RT-PCR. *Nucleic Acids Res.* **29,** e45
16. Tattikota, S. G., Rathjen, T., McAnulty, S. J., Wessels, H. H., Akerman, I., van de Bunt, M., Hausser, J., Esguerra, J. L., Musahl, A., Pandey, A. K., You, X., Chen, W., Herrera, P. L., Johnson, P. R., O'Carroll, D., Eliasson, L., Zavolan, M., Gloyn, A. L., Ferrer, J., Shalom-Feuerstein, R., Aberdam, D., and Poy, M. N. (2014) Argonaute2 mediates compensatory expansion of the pancreatic β cell. *Cell Metab.* **19,** 122–134
17. O'Byrne, S. M., Wongsiriroj, N., Libien, J., Vogel, S., Goldberg, I. J., Baehr, W., Palczewski, K., and Blaner, W. S. (2005) Retinoid absorption and storage is impaired in mice lacking lecithin:retinol acyltransferase (LRAT). *J. Biol. Chem.* **280,** 35647–35657
18. Ray, W. J., Bain, G., Yao, M., and Gottlieb, D. I. (1997) CYP26, a novel mammalian cytochrome P450, is induced by retinoic acid and defines a new family. *J. Biol. Chem.* **272,** 18702–18708
19. Gillespie, R. F., and Gudas, L. J. (2007) Retinoid regulated association of transcriptional co-regulators and the polycomb group protein SUZ12 with the retinoic acid response elements of Hoxa1, RARbeta(2), and Cyp26A1 in F9 embryonal carcinoma cells. *J. Mol. Biol.* **372,** 298–316
20. Durand, B., Saunders, M., Leroy, P., Leid, M., and Chambon, P. (1992) All-trans and 9-*cis*-retinoic acid induction of CRABPII transcription is mediated by RAR-RXR heterodimers bound to DR1 and DR2 repeated motifs. *Cell* **71,** 73–85
21. Ghyselinck, N. B., Båvik, C., Sapin, V., Mark, M., Bonnier, D., Hindelang, C., Dierich, A., Nilsson, C. B., Håkansson, H., Sauvant, P., Azaïs-Braesco, V., Frasson, M., Picaud, S., and Chambon, P. (1999) Cellular retinol-binding protein I is essential for vitamin A homeostasis. *EMBO J.* **18,** 4903–4914
22. Thatcher, J. E., and Isoherranen, N. (2009) The role of CYP26 enzymes in retinoic acid clearance. *Expert Opin. Drug Metab. Toxicol.* **5,** 875–886
23. Lotan, R. (2005) A crucial role for cellular retinol-binding protein I in retinoid signaling. *J. Natl. Cancer Inst.* **97,** 3–4
24. Niederreither, K., Abu-Abed, S., Schuhbaur, B., Petkovich, M., Chambon, P., and Dollé, P. (2002) Genetic evidence that oxidative derivatives of retinoic acid are not involved in retinoid signaling during mouse development. *Nat. Genet.* **31,** 84–88
25. Tannous-Khuri, L., and Talmage, D. A. (1997) Decreased cellular retinol-binding protein expression coincides with the loss of retinol responsiveness in rat cervical epithelial cells. *Exp. Cell Res.* **230,** 38–44
26. Nagy, N. E., Holven, K. B., Roos, N., Senoo, H., Kojima, N., Norum, K. R., and Blomhoff, R. (1997) Storage of vitamin A in extrahepatic stellate cells in normal rats. *J. Lipid Res.* **38,** 645–658
27. Haber, P. S., Keogh, G. W., Apte, M. V., Moran, C. S., Stewart, N. L., Crawford, D. H., Pirola, R. C., McCaughan, G. W., Ramm, G. A., and Wilson, J. S. (1999) Activation of pancreatic stellate cells in human and experimental pancreatic fibrosis. *Am. J. Pathol.* **155,** 1087–1095
28. Noy, N. (2010) Between death and survival: retinoic acid in regulation of apoptosis. *Annu. Rev. Nutr.* **30,** 201–217
29. Hengartner, M. O. (2000) The biochemistry of apoptosis. *Nature* **407,** 770–776
30. Kilimnik, G., Kim, A., Jo, J., Miller, K., and Hara, M. (2009) Quantification of pancreatic islet distribution in situ in mice. *Am. J. Physiol. Endocrinol. Metab.* **297,** E1331–E1338
31. Kim, A., Miller, K., Jo, J., Kilimnik, G., Wojcik, P., and Hara, M. (2009) Islet architecture: A comparative study. *Islets* **1,** 129–136
32. Jo, J., Hara, M., Ahlgren, U., Sorenson, R., and Periwal, V. (2012) Mathematical models of pancreatic islet size distributions. *Islets* **4,** 10–19
33. Chen, Y., Pan, F. C., Brandes, N., Afelik, S., Sölter, M., and Pieler, T. (2004) Retinoic acid signaling is essential for pancreas development and promotes endocrine at the expense of exocrine cell differentiation in Xenopus. *Dev. Biol.* **271,** 144–160
34. Gu, G., Dubauskaite, J., and Melton, D. A. (2002) Direct evidence for the pancreatic lineage: NGN3+ cells are islet progenitors and are distinct from duct progenitors. *Development* **129,** 2447–2457
35. Criscimanna, A., Speicher, J. A., Houshmand, G., Shiota, C., Prasadan, K., Ji, B., Logsdon, C. D., Gittes, G. K., and Esni, F. (2011) Duct cells contribute to regeneration of endocrine and acinar cells following pancreatic damage in adult mice. *Gastroenterology* **141,** 1451–1462, 1462.e1–6
36. Xu, X., D'Hoker, J., Stangé, G., Bonné, S., De Leu, N., Xiao, X., Van de Casteele, M., Mellitzer, G., Ling, Z., Pipeleers, D., Bouwens, L., Scharfmann, R., Gradwohl, G., and Heimberg, H. (2008) Beta cells can be generated from endogenous progenitors in injured adult mouse pancreas. *Cell* **132,** 197–207
37. Gradwohl, G., Dierich, A., LeMeur, M., and Guillemot, F. (2000) neurogenin3 is required for the development of the four endocrine cell lineages of the pancreas. *Proc. Natl. Acad. Sci. U.S.A.* **97,** 1607–1611
38. Al-Hasani, K., Pfeifer, A., Courtney, M., Ben-Othman, N., Gjernes, E., Vieira, A., Druelle, N., Avolio, F., Ravassard, P., Leuckx, G., Lacas-Gervais, S., Ambrosetti, D., Benizri, E., Hecksher-Sorensen, J., Gounon, P., Ferrer, J., Gradwohl, G., Heimberg, H., Mansouri, A., and Collombat, P. (2013) Adult duct-lining cells can reprogram into β-like cells able to counter repeated cycles of toxin-induced diabetes. *Dev Cell* **26,** 86–100
39. Van de Casteele, M., Leuckx, G., Baeyens, L., Cai, Y., Yuchi, Y., Coppens, V., De Groef, S., Eriksson, M., Svensson, C., Ahlgren, U., Ahnfelt-Rønne, J., Madsen, O. D., Waisman, A., Dor, Y., Jensen, J. N., and Heimberg, H. (2013) Neurogenin 3+ cells contribute to β-cell neogenesis and proliferation in injured adult mouse pancreas. *Cell Death Dis.* **4,** e523
40. Offield, M. F., Jetton, T. L., Labosky, P. A., Ray, M., Stein, R. W., Magnuson, M. A., Hogan, B. L., and Wright, C. V. (1996) PDX-1 is required for pancreatic outgrowth and differentiation of the rostral duodenum. *Development* **122,** 983–995
41. Holland, A. M., Góñez, L. J., Naselli, G., Macdonald, R. J., and Harrison, L. C. (2005) Conditional expression demonstrates the role of the homeodomain transcription factor Pdx1 in maintenance and regeneration of beta-cells in the adult pancreas. *Diabetes* **54,** 2586–2595
42. Kulkarni, R. N., Jhala, U. S., Winnay, J. N., Krajewski, S., Montminy, M., and Kahn, C. R. (2004) PDX-1 haploinsufficiency limits the compensatory islet hyperplasia that occurs in response to insulin resistance. *J. Clin. Invest.* **114,** 828–836
43. Brissova, M., Blaha, M., Spear, C., Nicholson, W., Radhika, A., Shiota, M., Charron, M. J., Wright, C. V., and Powers, A. C. (2005) Reduced PDX-1 expression impairs islet response to insulin resistance and worsens glucose homeostasis. *Am. J. Physiol. Endocrinol. Metab.* **288,** E707–E714
44. Talchai, C., Xuan, S., Kitamura, T., DePinho, R. A., and Accili, D. (2012) Generation of functional insulin-producing cells in the gut by Foxo1 ablation. *Nat. Genet.* **44,** 406–412
45. Berry, D. C., and Noy, N. (2009) All-*trans*-retinoic acid represses obesity and insulin resistance by activating both peroxisome proliferation-activated receptor beta/delta and retinoic acid receptor. *Mol. Cell. Biol.* **29,** 3286–3296

46. Schwarz, E. J., Reginato, M. J., Shao, D., Krakow, S. L., and Lazar, M. A. (1997) Retinoic acid blocks adipogenesis by inhibiting C/EBPbeta-mediated transcription. *Mol. Cell. Biol.* **17,** 1552–1561
47. Kim, S. C., Kim, C. K., Axe, D., Cook, A., Lee, M., Li, T., Smallwood, N., Chiang, J. Y., Hardwick, J. P., Moore, D. D., and Lee, Y. K. (2014) All-*trans*-retinoic acid ameliorates hepatic steatosis in mice by a novel transcriptional cascade. *Hepatology* **59,** 1750–1760
48. Graham, T. E., Yang, Q., Blüher, M., Hammarstedt, A., Ciaraldi, T. P., Henry, R. R., Wason, C. J., Oberbach, A., Jansson, P. A., Smith, U., and Kahn, B. B. (2006) Retinol-binding protein 4 and insulin resistance in lean, obese, and diabetic subjects. *N. Engl. J. Med.* **354,** 2552–2563
49. Masaki, T., Anan, F., Tsubone, T., Gotoh, K., Chiba, S., Katsuragi, I., Nawata, T., Kakuma, T., and Yoshimatsu, H. (2008) Retinol binding protein 4 concentrations are influenced by renal function in patients with type 2 diabetes mellitus. *Metabolism* **57,** 1340–1344
50. University of California, San Diego (2000) A randomized, double-blind study of the effects of fenretinide administered in subjects with obesity. In ClinicalTrials.gov, National Library of Medicine, Bethesda, MD
51. Chen, H., Charlat, O., Tartaglia, L. A., Woolf, E. A., Weng, X., Ellis, S. J., Lakey, N. D., Culpepper, J., Moore, K. J., Breitbart, R. E., Duyk, G. M., Tepper, R. I., and Morgenstern, J. P. (1996) Evidence that the diabetes gene encodes the leptin receptor: identification of a mutation in the leptin receptor gene in db/db mice. *Cell* **84,** 491–495
52. Puff, R., Dames, P., Weise, M., Göke, B., Seissler, J., Parhofer, K. G., and Lechner, A. (2011) Reduced proliferation and a high apoptotic frequency of pancreatic beta cells contribute to genetically-determined diabetes susceptibility of db/db BKS mice. *Horm Metab. Res.* **43,** 306–311
53. Kilimnik, G., Zhao, B., Jo, J., Periwal, V., Witkowski, P., Misawa, R., and Hara, M. (2011) Altered islet composition and disproportionate loss of large islets in patients with type 2 diabetes. *PLoS One* **6,** e27445
54. Wang, X., Misawa, R., Zielinski, M. C., Cowen, P., Jo, J., Periwal, V., Ricordi, C., Khan, A., Szust, J., Shen, J., Millis, J. M., Witkowski, P., and Hara, M. (2013) Regional differences in islet distribution in the human pancreas: preferential beta-cell loss in the head region in patients with type 2 diabetes. *PLoS One* **8,** e67454
55. Hull, R. L., Westermark, G. T., Westermark, P., and Kahn, S. E. (2004) Islet amyloid: a critical entity in the pathogenesis of type 2 diabetes. *J. Clin. Endocrinol. Metab.* **89,** 3629–3643
56. Li, Z., Karlsson, F. A., and Sandler, S. (2000) Islet loss and alpha cell expansion in type 1 diabetes induced by multiple low-dose streptozotocin administration in mice. *J. Endocrinol.* **165,** 93–99
57. Zhang, Y., Bone, R. N., Cui, W., Peng, J. B., Siegal, G. P., Wang, H., and Wu, H. (2012) Regeneration of pancreatic non-β endocrine cells in adult mice following a single diabetes-inducing dose of streptozotocin. *PLoS One* **7,** e36675
58. Krakowski, M. L., Kritzik, M. R., Jones, E. M., Krahl, T., Lee, J., Arnush, M., Gu, D., Mroczkowski, B., and Sarvetnick, N. (1999) Transgenic expression of epidermal growth factor and keratinocyte growth factor in beta-cells results in substantial morphological changes. *J. Endocrinol.* **162,** 167–175
59. Chung, C. H., Hao, E., Piran, R., Keinan, E., and Levine, F. (2010) Pancreatic β-cell neogenesis by direct conversion from mature α-cells. *Stem Cells* **28,** 1630–1638
60. Thorel, F., Népote, V., Avril, I., Kohno, K., Desgraz, R., Chera, S., and Herrera, P. L. (2010) Conversion of adult pancreatic alpha-cells to beta-cells after extreme beta-cell loss. *Nature* **464,** 1149–1154
61. Collombat, P., Hecksher-Sørensen, J., Krull, J., Berger, J., Riedel, D., Herrera, P. L., Serup, P., and Mansouri, A. (2007) Embryonic endocrine pancreas and mature beta cells acquire alpha and PP cell phenotypes upon Arx misexpression. *J. Clin. Invest.* **117,** 961–970